MESOSCOPIC PROTEIN RICH PHASES IN RIBONUCLEASE A SOLUTION

A Thesis

Presented to

the Faculty of the Department of Chemical and Biomolecular Engineering

University of Houston

In Partial Fulfillment

of the Requirements for the Degree

Masters of Science

in Chemical Engineering

by

Rajat Subhra Ghosh

December 2016

MESOSCOPIC PROTEIN RICH PHASES IN RIBONUCLEASE A SOLUTION

Rajat Subhra Ghosh

Approved:

Chair of the Committee
Peter G. Vekilov, Professor
Chemical and Biomolecular Engineering
Chemistry

Committee Members:

Vassiliy Lubchenko, Associate Professor
Chemistry

Jeffrey Rimer, Associate Professor
Chemical and Biomolecular Engineering

Suresh K. Khator, Associate Dean,
Cullen College of Engineering

Michael P. Harold, Chair,
Chemical and Biomolecular Engineering

ACKNOWLEDGEMENTS

I would like to thank my advisor Professor Peter G. Vekilov from the Chemical and Biomolecular Engineering department at the University of Houston for his constant support and feedback necessary for the completion of my project.

I would also like to take this opportunity to thank Dr. Vassiliy Lubchenko from the Chemistry department at the University of Houston and Dr. Jeffrey Rimer from the Chemical and Biomolecular Engineering department at the University of Houston for being a part of my committee and for insightful comments on my project.

I would like to thank my lab members for helping me with my experiments and giving valuable knowledge about various techniques that I had learnt during my stay in the lab.

Last but not the least, I would like to thank my parents for supporting and advising me in every way possible and giving me the will power to make it through.

MESOSCOPIC PROTEIN RICH PHASES IN RIBONUCLEASE A SOLUTION

An Abstract

of a

Thesis

Presented to

the Faculty of the Department of Chemical and Biomolecular Engineering

University of Houston

In Partial Fulfillment

of the Requirements for the Degree

Masters of Science

in Chemical Engineering

by

Rajat Subhra Ghosh

December 2016

ABSTRACT

Dense liquid phases called clusters exist in protein solutions and act as a precursor to crystal nucleation. Clusters have a narrow size distribution and submicron size. These clusters are present in a minor fraction of total protein, not affecting the properties of the solution, but are essential precursors for the nucleation of ordered species. The experiments here are done with acidic protein solution of Ribonuclease A (RNase A). Here we studied the effect of ionic strength, urea and temperature with the help of Brownian microscopy (BM), static light scattering (SLS), and several biochemical assays. The cluster size distribution was measured for three days with BM and revealed a consistently narrow size distribution through this time period, indicating stability of clusters. The clusters respond to the change in protein concentration, this change is exhibited as decrease in cluster volume fraction as the protein concentration was increased, indicating these clusters are not irreversible aggregates. The intermolecular forces were varied by changing the ionic strength with NaCl, $(NH_4)_2SO_4$ and CH_3COONa and quantified by measuring second virial coefficient by SLS. The data revealed that intermolecular repulsion decreases the cluster size and cluster volume fraction. The hydrophobic interactions between the exposed hydrophobic residues due to partial unfolding and solvent was studied by the addition of urea, a chaotropic agent that destroys the shell of structured water around protein molecules. Elman's assay was used to quantify the free thiols and the degree of unfolding was studied using ANS and ThT assays. The unfolding of protein by breaking disulphide bonds by heating showed an increase in cluster size and cluster volume fraction indicating the role of protein unfolding to aid the cluster formation. These experiments demonstrated the relevance of partial unfolding and intermolecular interactions in formation of clusters.

TABLE OF CONTENTS

LIST OF FIGURES

CHAPTER 1

INTRODUCTION

Proteins are large biomolecules that play many critical roles in the body. They do most of the work in cells and are required for the structure, function and regulation of body's tissues and organs. Proteins are made up of a definite arrangement of amino acids attached to one another in long chains. The importance of protein can be appreciated by discussing its functions. Depending upon the amino acids sequence and 3-dimensional spatial orientation, these can act as Antibody (Immunoglobulin G, IgG), Enzyme (Pepsin), Messenger (Insulin), Structural component (Collagens) and for Transport/Storage (Hemoglobin). The progress in molecular biology and its application to human medicine, agriculture, and industrial processes have been crucially dependent on a detailed knowledge of macromolecular structure at the atomic level.

In order to get a detailed structural information that provides insight into the molecular mechanisms underlying the function of bio-macromolecules, the technique that can be used and is the most reliable approach is X-ray diffraction of protein crystals. This technique requires the crystal to be of high quality (minimum defects) and size of crystal to be around 50-500 μm[1]. Crystallization of such large crystals with minimal defects becomes challenging and these problems have been discussed in literature[2,3].

The previous paragraphs elucidate the importance of Protein Crystallization and the need to understand the theory and mechanism behind crystallization. The crystallization of protein is complex and this is because of the various interactions that the protein experiences which effects the structural conformation. Interactions include hydrogen bonding, electrostatics, hydrophobic and steric hindrance. These interactions are highly

sensitive to the environment of the solution. Temperature, pH, ionic strength are a few parameters which changes the inter and intramolecular interactions of proteins[4-8].

Thermodynamics plays a key role in understanding the driving force behind crystallization and this analysis lead to the development of the Classical Nucleation theory by J.W. Gibbs in 1876[9,10]. For the any process to be thermodynamically favorable, ΔG has to be negative, applying this concept to the case of crystallization:

$$\Delta G_{cryst} = \Delta H_{cryst} - T\Delta S_{cryst} < 0, \qquad (1\text{-}1)$$

where, ΔH_{cryst} is the enthalpy change of crystallization, ΔS_{cryst} is the entropy change of crystallization, and T is absolute temperature. It is a careful balance of enthalpy and entropy.

Crystallization is a first order phase transition starting with nucleation. Nucleation determines the main properties of crystal population, including crystal polymorph, number of crystals and their size and size distribution[11]. Nucleation can be distinguished either as homogeneous and heterogeneous.

Homogeneous Nucleation:

The formation of a solid nucleus leads to a Gibbs free energy change,

$$\Delta G = G_2 - G_1 = -V_S(G_V^L - G_V^S) + A^{SL}\gamma^{SL}, \qquad (1\text{-}2)$$

where V_S is the volume of solid sphere, A^{SL} is the solid/liquid interfacial area, γ^{SL} is the solid/liquid interfacial energy and $\Delta G_V^L - G_V^S$ is the difference between the free energies per unit volume of solid and liquid. Equation (1-2) can be expressed as sum of two contributing factors,

1. $\Delta G_V = (G_V^L - G_V^S)$ is the driving force for the solidification which exists below the equilibrium melting temperature, T_m and from the Figure 1-1 we can see that ΔG_V <0

below melting temperature. At T_m, ΔG_V is zero and hence ΔS_V^m is $\Delta H_V^m / T_m$. For very small ΔT,

$$\Delta G_V = \frac{\Delta H_V^m \Delta T}{T_m}. \quad (1\text{-}3)$$

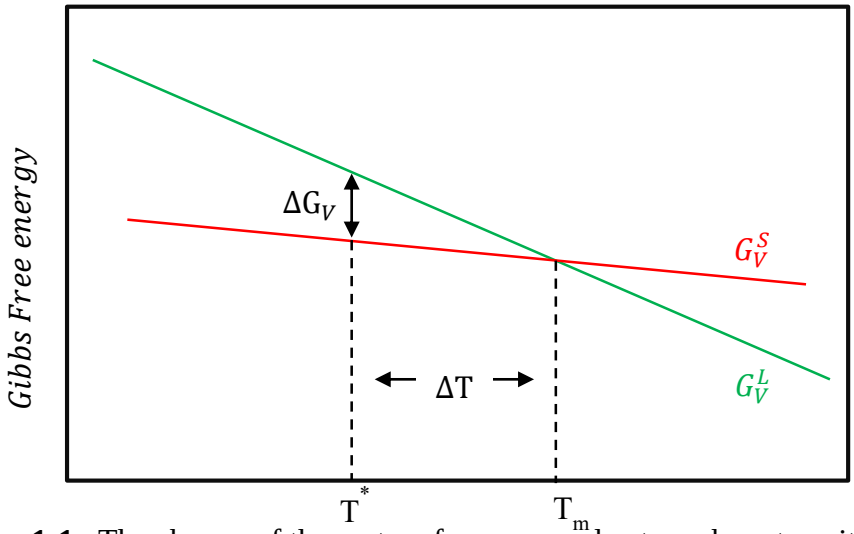

Figure 1-1. The change of the system free energy due to a phase transition.

2. Interfacial Energy (γ^{SL}) is the opposing energy due to the formation of new solid-liquid interface.

By assuming solid phase nucleates as spherical 'clusters' of radius, r, it can be shown from the equation (1-1), that the net excess free energy for a single nucleus, $\Delta G(r)$ is given by

$$\Delta G(r) = \frac{4}{3}\pi r^3 \Delta G_V + 4\pi r^2 \gamma^{SL} . \quad (1\text{-}4)$$

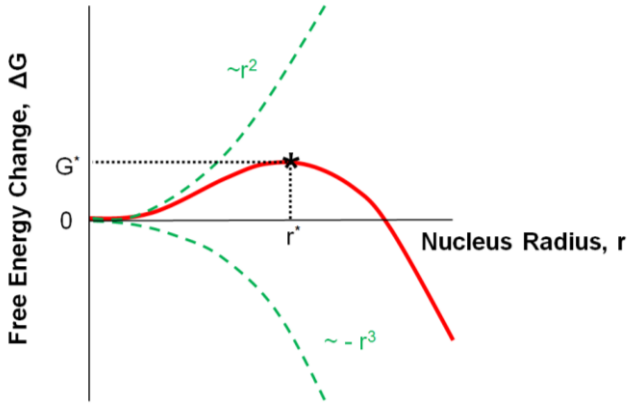

Figure 1-2. The change of the system free energy due to a formation of crystal nucleus.

For nucleus with a radius r>r*, the Gibbs free energy will decrease and if the nucleus grows. r* is the critical nucleus size and ΔG^* is the nucleation barrier.

To solve for the critical radius *r**, taking the derivative at the maximum of ΔG and we get,

$$r^* = \frac{2\gamma^{SL}}{\Delta G_V} \text{ and} \tag{1-5}$$

$$\Delta G^* = \frac{16\pi\gamma^{SL^3}}{3\Delta G_V{}^2}. \tag{1-6}$$

Heterogeneous Nucleation:

Heterogeneous nucleation takes place at preferential sites such as phase boundaries, surfaces or impurities like dust. At such sites, the effective surface energy is lower, thus diminishes the free energy barrier and facilitating nucleation.

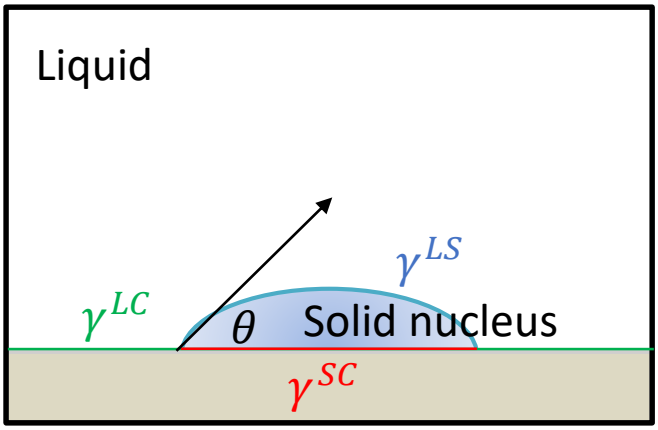

Figure 1-3. Schematic representation of Heterogeneous Nucleation

Consider the simple example as shown in the Figure 1-3, there are three interfacial energies, γ^{SL} is the interfacial energy of the Solid-Liquid surface, γ^{SC} is the interfacial energy of the Solid-Container surface and γ^{LC} is the interfacial energy of the Liquid-Container surface and balancing the interfacial tensions in the plan of container gives the wetting angle cos(θ) as $(\gamma^{LC} - \gamma^{SC})/\gamma^{SL}$.The formation of nucleus leads to the Gibbs free energy change,

$$\Delta G_{Hetero} = -V_S(G_V^L - G_V^S) + A^{SL}\gamma^{SL} + A^{SC}\gamma^{SC} - A^{SC}\gamma^{LC}\,, \tag{1-7}$$

and it can be shown that,

$$\Delta G_{Hetero} = \Delta G_{Homo} S(\theta), \tag{1-8}$$

where, $S(\theta)$ is $\frac{(2+\cos(\theta))(1-\cos(\theta))^2}{4} \leq 1$

In order to find the critical radius and critical Gibbs energy, take the derivative of Equation (1-7),

$$r^* = \frac{2\gamma^{SL}}{\Delta G_V} \quad \text{and} \tag{1-9}$$

$$\Delta G^* = \frac{16\pi\gamma^{SL^3}}{3\Delta G_V{}^2} S(\theta). \quad (1\text{-}10)$$

Comparison of Homogeneous and Heterogeneous nucleation can be shown using the Figure 1-4, which shows the nucleation barrier is significantly lower for heterogeneous nucleation due to wetting angle affecting the shape of nucleus.

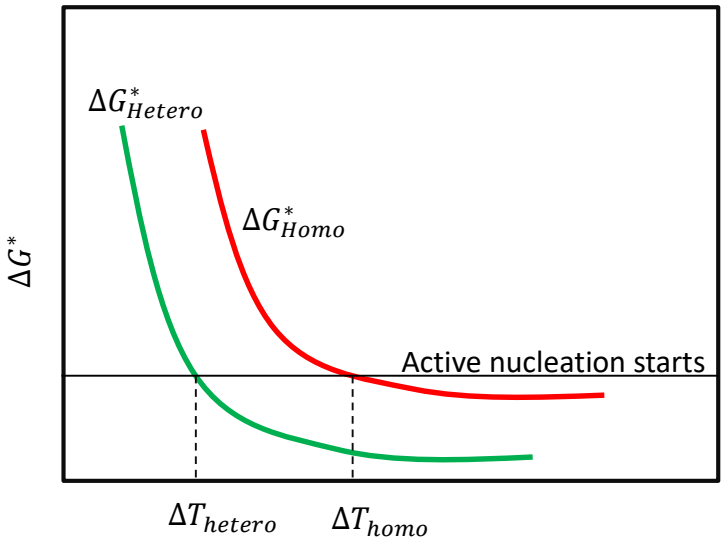

Figure 1-4. Critical Gibbs free energy comparisons of Homogeneous and Heterogeneous nucleation

Kinetics of Nucleation:

The nucleation rate J, is the number of nuclei which appears in a unit solution volume per unit time. It was postulated that in accordance with Arrhenius equation, $J = J_0 \exp\left(-\frac{\Delta G^*}{k_B T}\right)$, where k_B is the Boltzmann constant[12,13]. Based on the assumptions of Classical Nucleation theory, the final expression for the Nucleation Rate, J can be expressed as[14]

$$J = v^* Zn \exp\left(-\frac{\Delta G^*}{k_B T}\right), \quad (1\text{-}11)$$

where v^* is the rate of attachment of monomers to nucleus, Z is the Zeldovich factor, which accounts for the width of the free energy profile $\Delta G(n)$ in the vicinity of the maximum ΔG^* and n is the number density of molecules in the solution. A more refined equation of the nucleation rate is discussed below.

For nucleation to occur, the cluster size must be greater than the critical nucleus size, r^*, at which the activation barrier of ΔG^* is reached, and then there is additional barrier, ΔG_m which is the free energy spent for a monomer to cross the interface separating the nucleus and matrix. Hence rate of nucleation can be expressed as

$$J = A(T) * \exp\left(-\frac{\Delta G_m}{k_B T}\right) \exp\left(-\frac{\Delta G^*}{k_B T}\right), \quad (1\text{-}12)$$

where A(T) is the pre-exponential factor and is a function of n, critical radius, interfacial energy, number of surface atoms across the nucleus interface[15].

The experimental measurement of nucleation rates is challenging. In protein crystallization, the first measurements of nucleation rates were achieved in 2000 by Galkin and Vekilov[16]. Their experiments could separate heterogeneous nucleation from homogeneous, allowing the extraction of the steady-state rate of homogeneous nucleation from solution. the method required a protein solution to be loaded at a temperature chosen to prevent nucleation or liquid-liquid demixing. Then the temperature was lowered to a selected T_1 at which nucleation occurred. After a time period of Δt the temperature was raised from the nucleation temperature T_1 to the growth temperature T_2. At T_2, supersaturation was at levels where nucleation rate was almost eliminated but already formed crystals could grow to detectable sizes. This allows separation of the nucleation from the ensuing growth. After the growth stage, the nucleated crystals were

counted. To suppress undesired heterogeneous nucleation at the solution-air interface, the protein solution droplets were suspended in inert silicon oil.

The nucleation rates found from such experiments as performed by Galkin and Vekilov[16] had certain peculiarities and the most important of the discrepancy is that, Classical Nucleation theory overestimates the nucleation rate by 10 orders of magnitude this is due to the over estimation of the pre-exponential factor in the Equation (1-11) and

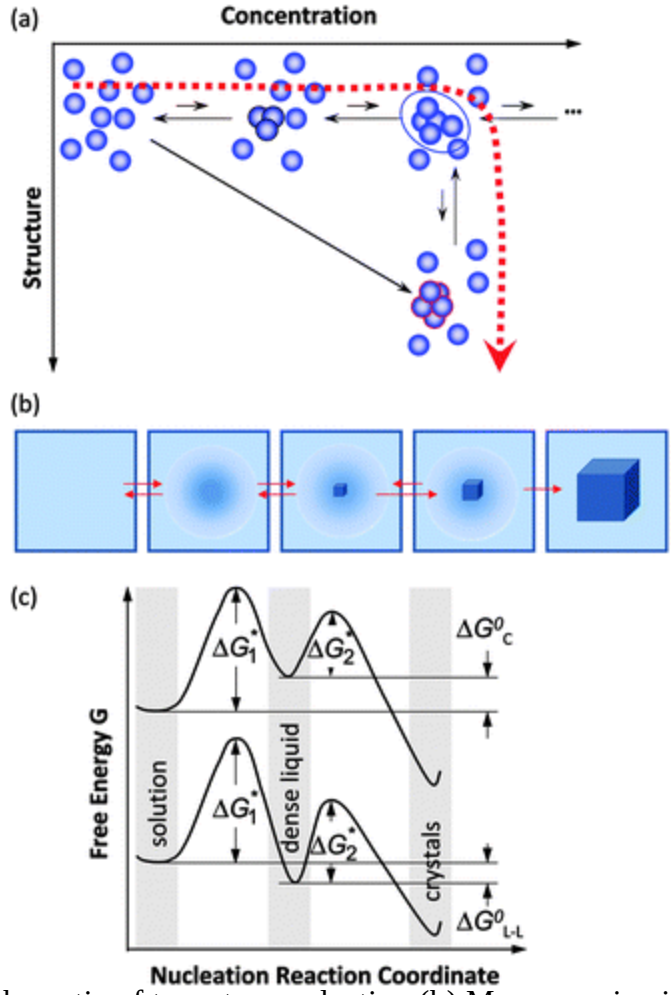

Figure 1.5. (a) Schematic of two step nucleation (b) Macroscopic view point of events along dashed lines in (a). (c) Free energy along two possible pathways for nucleation of crystals from solution[22]

also that the nucleation rate is not a monotonic function, the nucleation increases and then decreases. The main idea that was proposed that crystal nucleation occurs inside the

metastable mesoscopic clusters of dense protein liquid. According to this mechanism, crystal nuclei assemble within preexisting protein-rich clusters rather than from molecules in the dilute solution. The surface free energy at the interface between the crystal and the solution is significantly higher than at the interface between the crystal and the dense liquid, the barrier for nucleation of crystals from the solution would be much higher. This would lead to much slower nucleation of crystals directly from the solution than inside the clusters. Thus, the protein crystal nucleation follows the two-step mechanism of nucleation because it provides for faster rate of the solution to crystal phase transition and in this way for faster decrease of the free energy of the system, which corresponds to faster increase of the entropy[12,16].

The evidence of metastable dense liquid clusters comes from the monitoring of three hemoglobin variants, oxy-HbA, oxy-HbS, and deoxy-HbS 66, and protein synthase and lysozyme, by Dynamic Light Scattering and Atomic force microscopy[12,18,19].

Properties of Mesoscopic Clusters[20]:

1. Cluster diameters vary from 100 nm for relatively small lysozyme to several hundred nanometers for larger proteins. The cluster radius stays relatively steady over a prolonged periods of time
2. The number density n_2 of the dense liquid clusters and the fraction of the total solution volume φ_2 they occupy are evaluated from the amplitudes A_1 and A_2 of the intensity distribution function[21] as

$$n_2 = \frac{A_2}{A_1}\frac{1}{P(qR_2)f(C_1)}\frac{\left(\frac{\partial n}{\partial C_2}\right)_{T,\mu}}{\left(\frac{\partial n}{\partial C_1}\right)_{T,\mu}}\left(\frac{\rho_1}{\rho_2}\right)^2\left(\frac{R_1}{R_2}\right)^6 n_1 \quad \text{and} \tag{1-13}$$

$$\varphi_2 = \frac{A_2}{A_1}\frac{1}{P(qR_2)f(C_1)}\frac{\left(\frac{\partial n}{\partial C_2}\right)_{T,\mu}}{\left(\frac{\partial n}{\partial C_1}\right)_{T,\mu}}\left(\frac{\rho_1}{\rho_2}\right)^2\left(\frac{R_1}{R_2}\right)^3\varphi_1\,, \qquad (1\text{-}14)$$

where $P(qR_2)$ is the shape factor for the clusters of radius R_2, q is the scattering vector, $C_{1,2}$ is the concentration of monomers and clusters correspondingly, $f(C_1)$ is a virial expansion containing the coefficients of the solution osmotic compressibility, $\left(\frac{\partial n}{\partial C_{1,2}}\right)_{T,\mu}$ are the refractive index increments at constant temperature and chemical potential of monomers and clusters correspondingly, $\rho_{1,2}$ are the densities of monomers and clusters. The cluster occupies a very small volume fraction ranging from 10^{-7} to 10^{-3} of total volume.

3. Free energy cost is around $10k_bT$. Due to high free energy excess, clusters hold only 10^{-5} to 10^{-3} of total soluble protein
4. Consists of transient protein oligomers and monomers. Clusters results from interplay of monomer influx, oligomer formation and oligomer outflow and decay[22] , the schematic is shown in Figure 1-5.
5. The radius of cluster is given by, $R_2 = \sqrt{\frac{D_{oligomer}}{k_{oligomer}}}$

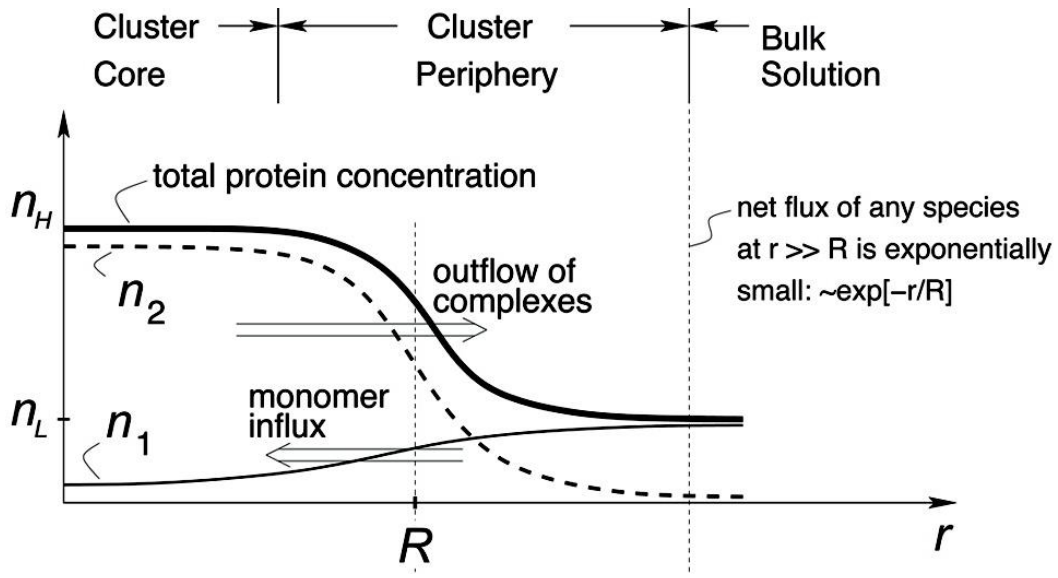

Figure 1-6. Schematic of concentration profiles in a cluster. n_L: total protein concentration in the bulk solution. n_H: total protein concentration in the cluster core. r: distance from center of cluster.

It is important to understand the mechanism behind the formation of transient complexes, which leads to the existence of mesoscopic clusters. The transient complexes of importance are the dimers formed by either domain swapping or by partial protein unfolding of protein monomers. In order to investigate the formation of such dimers, it would be suitable to work with a protein which has very high structural flexibility and has the ability to form various oligomeric species under very mild conditions. The protein which has such high flexibility without the loss of protein activity is Ribonuclease A (RNase A)[23-27].

RNase A is a small protein. This enzyme is secreted by exocrine cells of the bovine pancreas and has 124 amino acid residues. RNase A contains 19 of the 20 natural amino acids, lacking in tryptophan. The molecular formula for the native, uncharged enzyme is $C_{575}H_{907}N_{171}O_{192}S_{12}$. The formula corresponds to a molecular mass of 13686 Da with a pI of 9.6. The overall shape of the enzyme resembles that of a kidney, with the active residues lying in the cleft. The predominant elements of secondary structure are a long four-stranded

anti parallel β-sheet and three short α-helixes. The enzyme is crosslinked by four disulphide bonds which involve all eight of its cysteine residues. The peptide bonds preceding two of the four proline residues are in the Cis conformation[23-27].

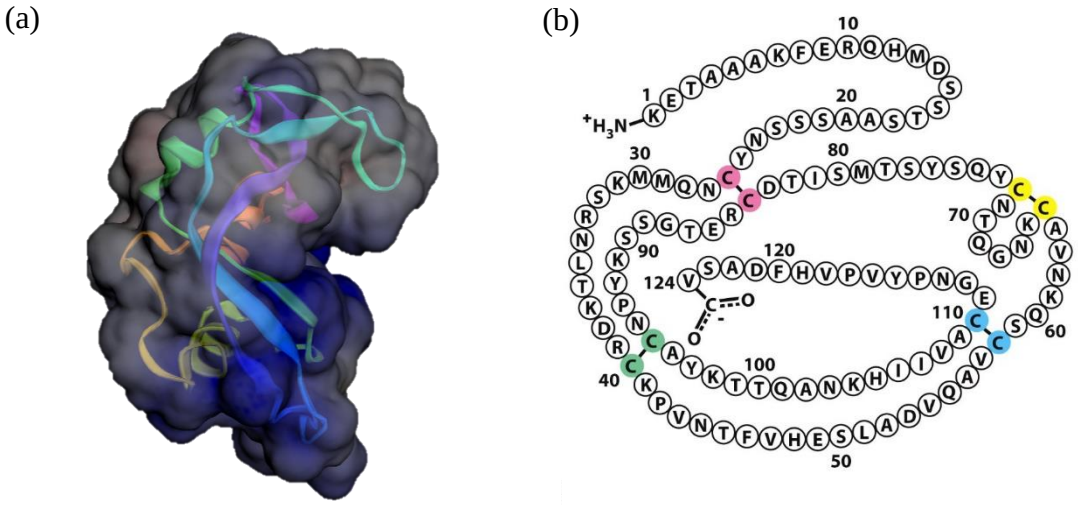

Figure 1-7. (a) The 3D structure of RNase A, shows the distinct kidney shaped structure. (b) Primary structure of RNase A, showcasing the arrangement of amino acid residues and the location of di-sulfide bonds.

RNase A has two domains, known as the N- Terminus (Residues 1-15) and the C- Terminus (Residues 116-124). The N -terminus consists of the first α-helix and the C- Terminus end consists of the β-sheet. RNase can form 3 different domain swapped structures, one with opening of N- Terminus, second with the opening of C- Terminus and the third when both N and C terminus are open. It must be noted that no disulphide bonds are broken during domain swapping.

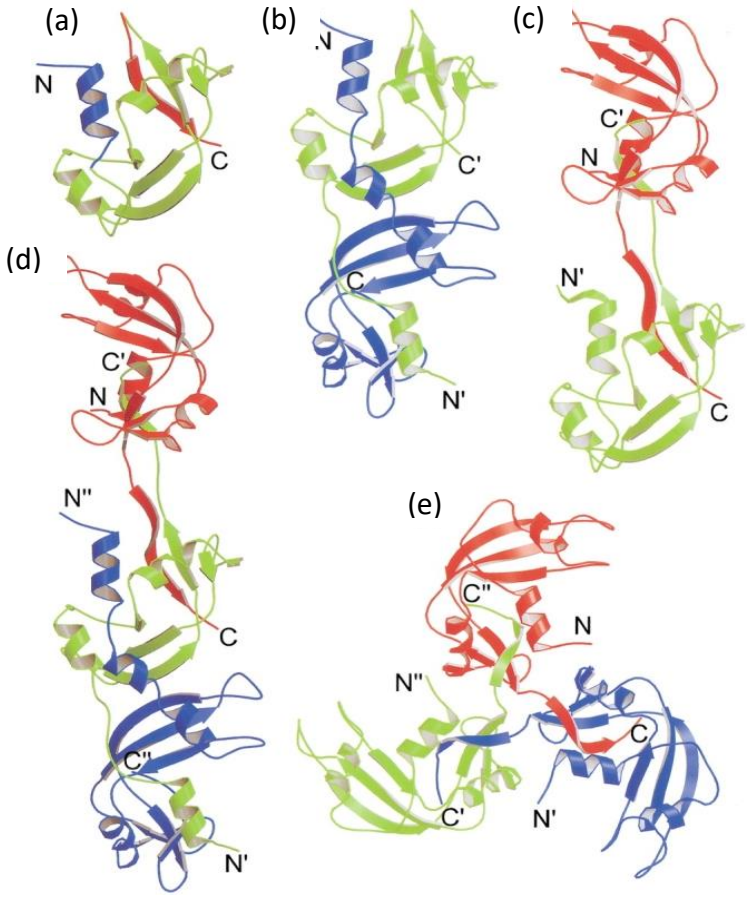

Figure 1-8. Ribbon diagrams of the structures of the RNase A monomer (a), the minor dimer (b), the major dimer (c), the major trimer model (d), and the minor trimer (e). The N- and C-termini are labelled[23].

These oligomeric species of RNase A are very stable in nature. As shown in the Figure 1-7, it shows there exists, two types of dimers,

1. N domain swapped dimer: This is formed by the swapping of the N-termini of each monomer (PDB entry 1A2W). Figure 1-7(b) shows the minor, less basic RNase A dimer, for which crystals were obtained and the structure solved in 1998 by Liu, Hart, Schlunegger and Eisenberg[28]. The N-terminal helix (residues 1–15) of each monomer is swapped into the major domain (residues 23–124) of the second monomer. The two subunits of this dimer interact through their three-stranded β-

sheets, forming a six-stranded sheet across the interface of the dimer. This is the new between the two subunits of the dimer, and is not present in the monomer of RNase A. The interface between the two subunits (the 'open interface') is formed by the two N-terminal α-helices (residues 24–33), and is stabilized by two disulphide bonds existing between Cys-31 and Cys-32 of each subunit.

2. C domain swapped dimer: The C-dimer is formed by the swapping of the C-termini of each monomer (PDB entry 1F0V). It represents the second and significantly more abundant RNase A dimer, the structure of which (Figure 1-7(c)). This dimer, called the major or more basic dimer is formed by the swapping of the C-terminal β-strand of each RNase A monomer (residues 116–124), producing a molecule whose size is larger than that of the N-dimer. While its hinge loop, i.e. the segment linking the two swapping domains, is shorter (amino acids 112–115) than that of the N-dimer (residues 16–22). The more elongated structure of the C-dimer exposes more positive charges as compared with the N-dimer.[24]

RNase A, can form other higher oligomeric forms[24] as shown in Figure 1-7. The N-terminal helix and the C-terminal strand that are swapped in the oligomers are colored in blue and red, respectively, in the monomer (a). The minor dimer (b) swaps the N-terminal helix, whereas the major dimer (c) swaps the C-terminal strand. Both types of swapping take place in the major trimer model (d): The green subunit swaps the C-terminal strand with the red subunit and swaps the N-terminal helix with the blue subunit. The minor trimer (e) is 3D domain-swapped at the C-terminal strands[23]All these oligomers are a result of domain swapping. These oligomeric forms are less abundant than compared to the dimers formed and these are less stable compared to dimers. It has been reported in literature, that

higher order oligomers such as trimers, tetramers, pentamers dissociate to lower oligomeric forms[26].

In my work, I have used RNase A, as a protein to study the formation of clusters in non-crystallizing conditions as in crystallizing conditions these clusters leads to the formation of nuclei and form crystals. Non-Crystallizing condition is necessary to inhibit the growth of crystals within these dense liquid clusters in order to understand the properties of mesoscopic clusters. Various parameters which are known to effect the size, number and volume fraction of clusters were changed to get an insight of mechanism of cluster formation and answer questions whether domain swapped dimers of RNase A leads to cluster formation, whether there is partial unfolding of RNase taking place instead via breaking of di-sulphide bonds which leads to cluster formation. The following parameters were varied:

1. Ionic Strength
2. Temperature
3. Effect of denaturing agent(Urea)

With the aid of Brownian microscopy, Chromatography, Gels and Biological assays an attempt was made to discuss and get a picture of the mechanism behind Cluster formation and the experimental techniques is explained in Chapter 2 of this document. The results and discussions from the above mentioned experiments are discussed in Chapter 3 and conclusions are made in Chapter 4. The future work of these experiments are discussed in Chapter 5.

CHAPTER 2

PRINCIPAL EXPERIMENTAL TECHNIQUES

2-1. Brownian Microscopy

Brownian microscopy has been used here to characterize the size and volume fraction of clusters. This technique uses the light scattering as a way to detect the large clusters through a camera. The clusters follow the Brownian motion and this can be related to Diffusivity(D) of cluster.

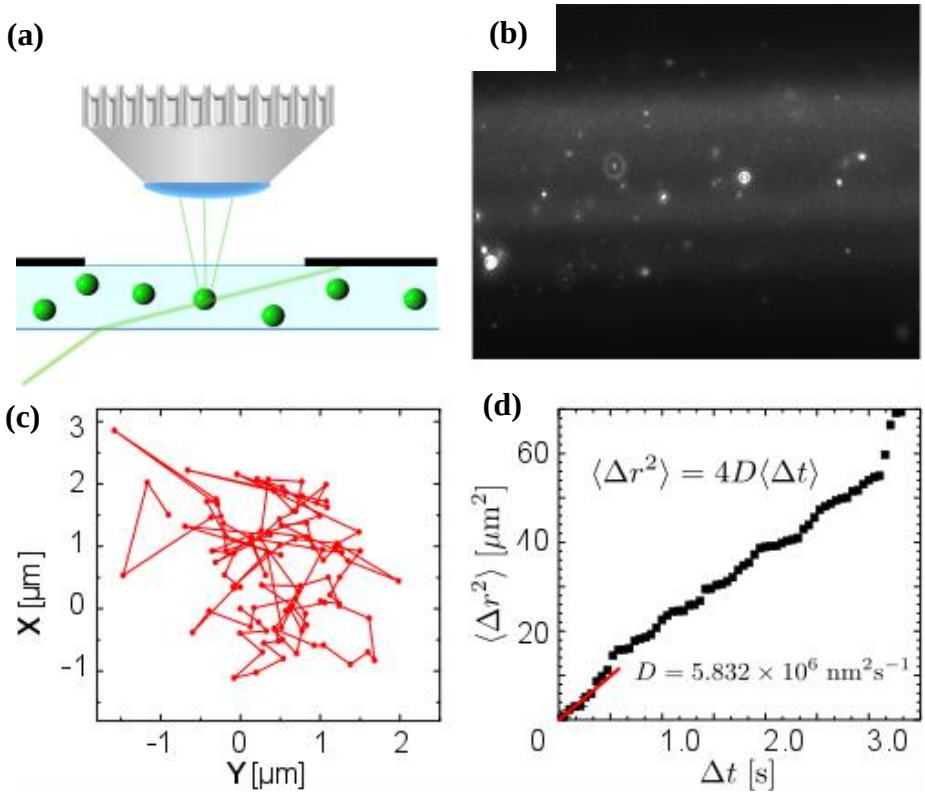

Figure 2-1. Cluster characterization by Brownian microscopy. **(a)**Schematic of the BM setup **(b)** A typical BM image **(c)** Cluster trajectory showing Brownian motion. (**d**) Diffusivity calculation from Equation (2-2).

Using a tracking software, the trajectories of Clusters following Brownian motion can be extracted in terms of X-Y co-ordinate system. After having the coordinates of all

the particles, the displacement is then squared and averaged over the number of steps 'n' plotted against time. The following equations,

$$\Delta r_i^2(\Delta t) = \left(\Delta x_i(\Delta t)\right)^2 + \left(\Delta y_i(\Delta t)\right)^2 \text{ and} \quad (2\text{-}1)$$

$$< (\Delta \boldsymbol{r}(\Delta \boldsymbol{t}))^{\boldsymbol{2}} > = \frac{1}{n}\sum_i^n \Delta r_i^2(\Delta t) = 4D < \Delta t > \quad (2\text{-}2)$$

allows the calculation of Diffusivity. Using Stokes-Einstein equation the radius of the cluster can be calculated.

Nanosight LM10-HS microscope (Nanosight Ltd, currently Malvern Instruments, USA) was used to examine the Brownian motion of individual clusters in the tested solutions. A solution sample was loaded in a thermostatically controlled cuvette of volume ~0.3 ml and depth 0.5 mm. The solution was illuminated by a laser beam configured so that it does not enter the objective lens of an observation microscope, Fig. 2-1 (a). The observation volume is determined by the focal depth of the objective lens and the view field of the microscope, and is typically 120 × 80 × 5 μm^3 (width × length × height). A 20× lens transfers the entire picture to a sensitive CMOS camera that records a movie of clusters undergoing Brownian motion. The rate of movie acquisition depends on camera settings and in our experiments it was about 25 fps unless it is noted otherwise. Each frame of the movie is an image of clusters as bright white spots on a dark background.

2-2. Static light scattering

Static Light Scattering (SLS) is an optical technique that measures the intensity of the scattered light in dependence of the scattering angle to obtain information on the scattering source.

A typical application is the determination of the weight average molecular weight Mw of a macromolecule such as a polymer or a protein. Other popular applications are the

measurement of the radius of gyration R_g or the form and structure factor. By measuring the scattering intensity for one macromolecule at various concentrations, the second virial coefficient B_2, can be calculated.

SLS has been used here to get information about the pairwise interactions in the protein solution. This technique gives information about the type of interactions between the proteins in the solution based on the second virial coefficient. The SLS data was collected by ALV light scattering device equipped with He-Ne laser (λ = 632.8 nm, 35 mW) and ALV-5000/EPP Multiple tau Digital Correlator (ALV-Gmbh, Langen, Germany). During the experiment, protein solutions were held in cylindrical cuvettes of volume from 0.5 to 1 ml at 20^0C.

The scattered intensity is collected at 90^0. For molecules in the dilute solution regime the simplified scattering equation is shown below.

$$\frac{Kc}{R_\theta} = \frac{1}{M_w} + 2B_2c, \tag{2-3}$$

where $R_\theta = I_\theta / I_0$ is a Rayleigh ratio of the scattered to the incident light intensity, c is the protein concentration, $K = \frac{1}{N_A}\left(\frac{2\pi n_0}{\lambda^2}\right)^2\left(\frac{dn}{dc}\right)^2$ is an optical constant, N_A is the Avogadro number, n_0 = 1.331 is the refractive index of the solvent at the wavelength of the laser beam, assumed to be equal to that of water, dn/dc = 0.199±0.003 ml g^{-1} is the refractive index increment of the solutions. In Debye plots, the slope of the graph gives the value of second virial coefficient(B_2) and the intercept gives the information about the Molecular weight(M_w) of the sample from Equation 2-3. A positive value of B_2 indicates the interactions are repulsive and negative value of B_2 indicates attractive interactions.

2-3. Ellman's Assay

The purpose of this assay is to quantify the number of free thiol groups, which indicates the broken disulphide bonds in the protein. This helps in assessing the role of disulphide bonds in cluster formation. The assay is based on the following reaction:

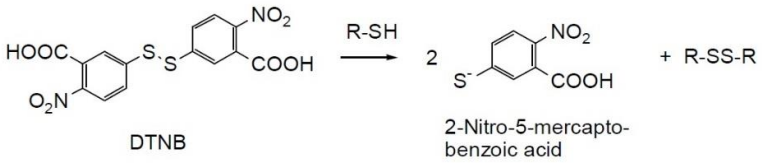

Thiol reacts with DTNB, cleaving the disulphide bond to give 2-Nitro-5-mercaptobenzoic acid(TNB^-) which ionizes to TNB^{2-} in water at neutral and alkaline pH. TNB^{2-} has a yellow color. This reaction is rapid and stoichiometric. TNB^{2-} is quantified in a spectrophotometer by measuring the absorbance of visible light at 412 nm with the extinction coefficient of 13600 $M^{-1}cm^{-1}$. A calibration as show in Figure 2-2 is plotted and later used to quantify the free thiol concentration in protein solutions based on protocol given by ThermoFischer for Ellman's reagent(DTNB).

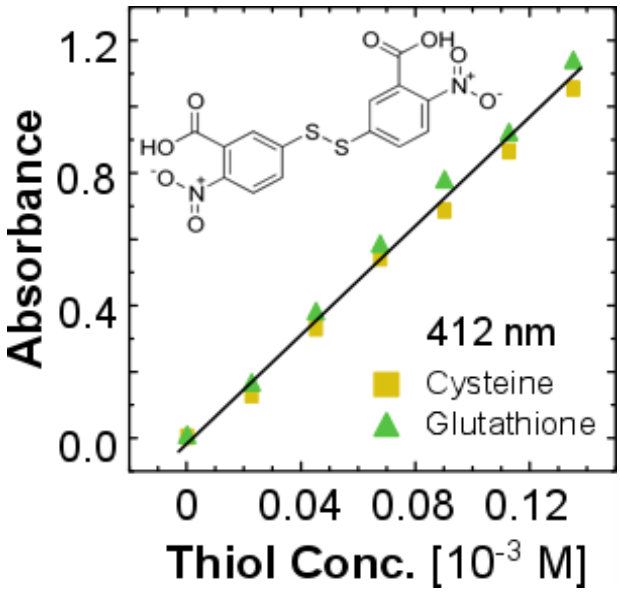

Figure 2-2. Free thiol Calibration curve

For the experiments, DTNB was purchased from Sigma Aldrich and a 8 $mgml^{-1}$ solution was prepared by mixing it in 20mM HEPES pH 7.8 and filtered using 0.2µm Teflon filters before use. The protein sample for which the thiol concentration was to be determined was filtered using 0.2µm Teflon filters. For the assay a transparent flat bottom 96 black well plate was used. For the assay 194µl of protein and 6µl of DTNB solution were pipetted carefully into the well. The absorbance was read using Infinite 200 PRO microplate reader(TECAN). The read absorbance was matched against the Calibration Curve (Figure 2-2) to evaluate the free thiol concentration in the protein. A blank is used, where instead of protein sample, the buffer in which protein solution was prepared to remove the effect of buffer on absorbance.

2-4. Thioflavin T Spectroscopic Assay

This assay has been used to characterize the unfolding of proteins in the given environment. Thioflavin T is a benzothiazole salt obtained by the methylation of dehydrothiotoluidine with methanol in the presence of hydrochloric acid. The dye is widely used to visualize and quantify the presence of misfolded protein aggregates called amyloid, both in vitro and in vivo (e.g., plaques composed of amyloid beta found in the brains of Alzheimer's disease patients). When it binds to beta sheet-rich structures, such as those in amyloid aggregates, the dye displays enhanced fluorescence and a characteristic red shift of its emission spectrum. In Figure 2-3(b) ThT is bound to an amyloid like oligomer which has high Beta sheet content. For the purpose of my work, higher signal from Beta sheet indicates unfolding of my protein. A higher fluorescent intensity indicates higher unfolding in the protein system.

(a) 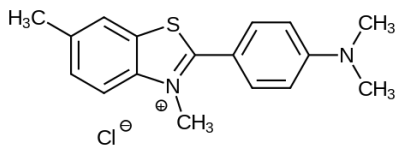

(b) 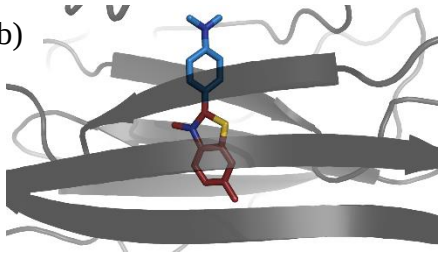

Figure 2-3. (a)Thioflavin T structure (b) Interaction of ThT with a highly ordered Beta sheet amyloid aggregate (shown in grey).

For experiments, Thiofalvin T was purchased from Sigma Aldrich and a solution of 6mM ThT was prepared using 20mM HEPES at pH 7.8. The ThT solution was filtered using 0.2µm Teflon filter. The protein sample for which the thiol concentration was to be determined was filtered using 0.2µm Teflon filters. For the assay a transparent flat bottom 96 black well plate was used. For the assay 199µl of protein and 1µl of ThT solution were pipetted carefully into the well. The fluorescence response to excitation at 442 nm was recorded between 472nm to 650 nm using Infinite 200 PRO microplate reader(TECAN).

2-4. ANS Spectroscopic Assay

ANS has sulfonated naphthalene with aniline group, the naphthalene backbone and aniline ring are hydrophobic, but the sulfonated group has a negative charge. The amide group at the aniline ring contains an amide, which can provide electron for hydrogen bond formation with a protein.

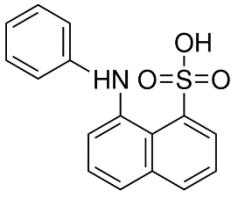

Figure 2-4. 8-Anilinonaphthalene-1-sulfonic acid(ANS)

The sulfonated group helps in interaction with positively charged amino acids such as lysine, arginine and histidine. Aromatic rings stabilize the binding with non-polar sides of proteins. In the native state of protein, hydrophobic residues are generally hidden inside except for ligand binding sites, proteins have hydrophilic or polar amino acids on the surface. When proteins are in denaturing condition, proteins may expose some of the hydrophobic residues on their surface. This method helps in detection of totally denatured protein. Binding of ANS to proteins requires both the ionic interaction of sulfonate with positively charged amino acids and the hydrophobic interactions of aromatic rings with hydrophobic residues in an oriented manner.

For experiments, ANS was purchased from Sigma Aldrich and a solution of 26mM ANS was prepared using 20mM HEPES at pH 7.8. The ANS solution was filtered using 0.2µm Teflon filter. The protein sample for which the thiol concentration was to be determined was filtered using 0.2µm Teflon filters. For the assay a transparent flat bottom 96 black well plate was used. For the assay 199µl of protein and 1µl of ANS solution were pipetted carefully into the well. The fluorescence response to excitation at 442 nm was recorded between 472nm to 650 nm using Infinite 200 PRO microplate reader(TECAN).

CHAPTER 3

RESULTS AND DISCUSSIONS

The two step nucleation theory which overcomes the shortfalls of the classical nucleation theory, indicates the presence of dense liquid droplets called Clusters. These clusters act as a precursor to nucleation. The presence of these dense liquid droplets or clusters has been shown for Lysozyme and Hemoglobin. These clusters leading to nucleation has been extensively studied in the case for the protein Lysozyme.

Ribonuclease A (RNase A) has a high structural flexibility and due to this distinct feature for RNase A, it might form clusters. Clusters are not aggregates of proteins. It becomes important to establish beyond a reasonable doubt, that RNase A forms clusters and not aggregates in environment studied and also to study the cluster properties.

3-1 Materials and methods

Reagents: Ribonuclease A (RNase A) was purchased from Sigma Alridch (R5125-500 mg) as the protein. Other reagents include Sodium Chloride, Ammonium Sulfate, Sodium Acetate and Urea for various experiments. For the assays, DTNB, ThT and ANS were purchased from the Sigma Aldrich.

Methods: To determine the radius of cluster and Cluster volume, Brownian Microscopy has been used. Assays has been used here to find the role of partial unfolding and disulphide bonds which includes Ellman's Assay, Thioflavin T Assay and ANS assay. The techniques have been described in the Chapter 2.

3-2 Results and discussions

RNase A is known to form oligomers and it is important to distinguish this from clusters. Clusters are known to be stable for a long time and have a monodispersed size distribution. The experiments were done in under saturated conditions. The concentration of RNase A was chosen at 2 $mgml^{-1}$ and was prepared in 100 mM Sodium Acetate buffer at pH 5.5. The pI of RNase A is 9.6 and at pH of 5.5, the protein is positively charged in the solution. The protein solution was filtered using a 0.2 μm Teflon filters. The solution was loaded into the cuvette of Nanosight (specifications as discussed in Chapter 2).

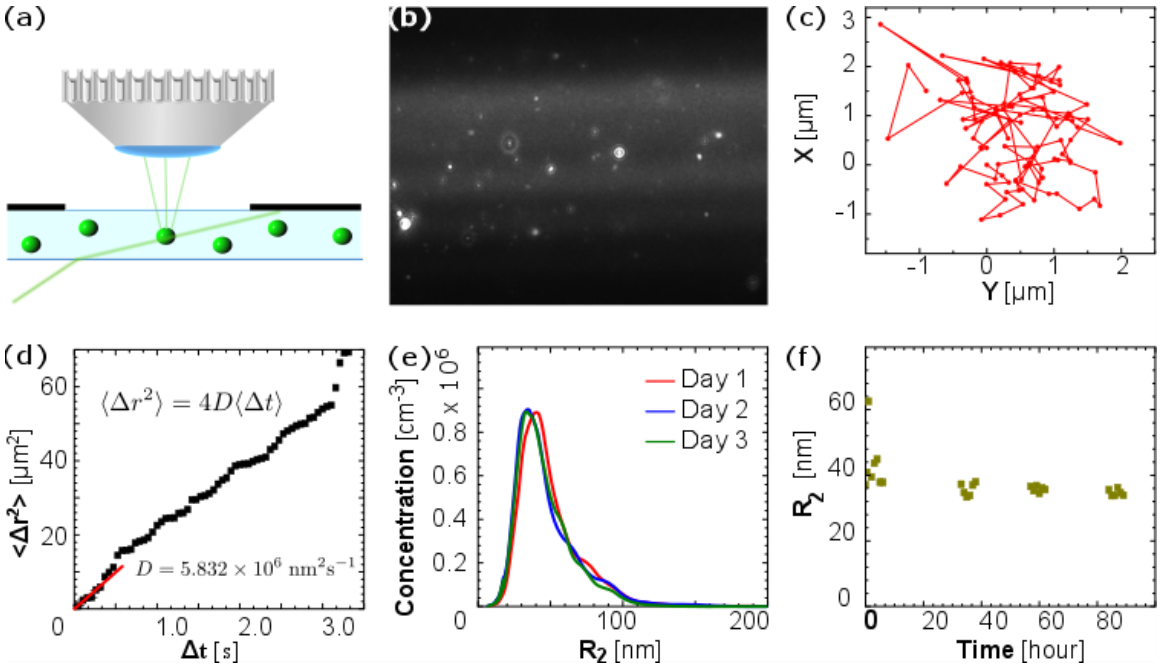

Figure 3-1. **(a)**Schematic of the BM setup **(b)** A typical BM image **(c)** Cluster Trajectory showing Brownian motion. (**d**) Diffusivity calculation **(e)** Cluster size distribution over time **(f)** Average size of clusters over time.

The principle of Brownian Microscopy as discussed in Chapter 2, uses the concept of Brownian motion and relating it to the Diffusivity. This value of diffusivity is used to determine the radius with the help of the Stokes-Einstein equation. The results of the

experiment with 2 $mgml^{-1}$ is shown in Figure 3-1. The following observations can be drawn:

1. The size distribution as shown in Figure 3-1(e) gives a fairly monodispersed distribution, which a characteristic property of clusters.
2. The average size distribution as shown in Figure 3-1(f) shows that radius remains constant for long period of time, here the experiments were done for 93 hours under the conditions of experiments as discussed in the previous paragraph.

The above experiment concludes about the monodispersed property and stability of the species observed using Nanosight.

Another experiment was done to check if the species observed using Nanosight were aggregates of the protein RNase A. In this experiment the concentration of protein RNase A was varied from 6 $mgml^{-1}$ to 1.5 $mgml^{-1}$ in the same Buffer of 100 mM Sodium Acetate at pH 5.5. The purpose of these experiments were to check if these species, are dead. Here the term dead has been used to mean whether these species respond to any changes in environment of experiments. It must be noted that, two types of symbols have been used here, this represents that the experiments were done in two ways. First individual solutions of specified protein concentrations were prepared and then analyzed using Nanosight. Second the protein solution of 6 $mgml^{-1}$ was diluted by adding 100 mM Sodium Acetate, pH 5.5 and later analyzed using Nanosight.

The results of this experiment has been shown in Figure 3-2. There are two parameters which were obtained from above experiments. The average radius and ratio of volume fraction of clusters to volume fraction of protein at that particular concentration

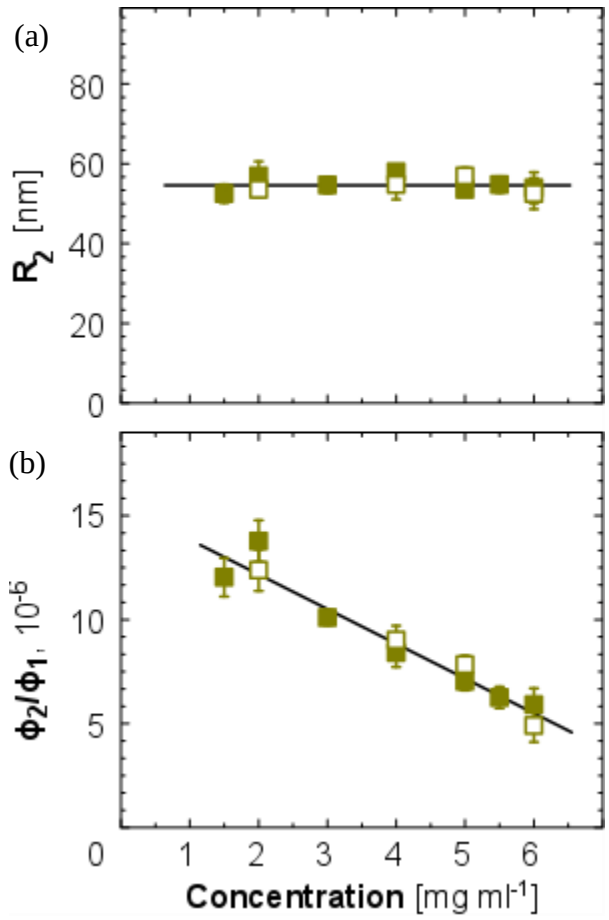

Figure 3-2. (a) Average Cluster radius as a function of Protein concentration (b) Ratio of volume fraction of clusters to monomeric protein in the solution as protein concentration is changed in the solution.

were the two parameters. The volume fraction of clusters can be calculated from the size distribution of these species similar to Figure 3-1(e), which gives the data of concentration which is a function of radius (f(r)) of clusters in terms of number per cm^{-3} of the protein solution. Assuming the volume of each cluster as spherical,

$$\varphi_2 = \sum \frac{4}{3}\pi r^3 f(r), \tag{3-1}$$

where 'r' is the radius of cluster and f(r) is the number concentration which is followed from the Figure 3-1(e). The volume fraction of monomeric protein in the solution for a particular concentration as 'c' $mgml^{-1}$ is given by,

$$\varphi_1 = \frac{c}{\rho}, \tag{3-2}$$

where ρ is the protein density in monomer which is around 1.18 gcm^{-3}. The following observations can be drawn from the results:

1. The average radius of clusters as protein concentration was varied is constant which implies that cluster radius of RNase A does not depend of protein concentration. The average radius of RNase A cluster is around 55 nm and stays constant within the range of error bars.
2. The ratio of volume fraction of clusters to protein monomers in RNase protein solution increases as the solution is diluted as shown in Figure 3-2(b).

From the above observations, it is safe to say the species observed are clusters and not aggregates. As if these were aggregates, the ratio φ_2/φ_1 would increase. Aggregation increases with increase in protein concentration. But here it shows the opposite trend. A further result that can be drawn is that, φ_2/φ_1 is in the range of 10^{-6} which is a very small fraction indicating that existence of these clusters are thermodynamically not favorable. This implies that equilibrium is shifted heavily towards the protein monomers and hence as protein concentration is increase the volume fraction of clusters with respect to protein concentration in the solution decreases. This is just an attempt to explain the trend of φ_2/φ_1.

The above two experiments suggest that the species observed here are clusters of RNase A. The protein at pH 5.5 is a highly charged species and this brings to the second part of experimentation to investigate the effect of ionic strength of solution. The ionic strength of solution has been changed by adding salts or by changing the buffer concentration. For the purpose of experiments, the concentration of Ribonuclease A

(RNase A) is 2 $mgml^{-1}$ in protein solution. Buffer used for all experiments is 100mM Sodium Acetate pH 5.5. Ionic strength of protein solution was changed using Sodium Chloride, Ammonium Sulfate or by changing buffer concentration. The residual ionic strength from 100 mM Sodium Acetate with pKa 4.76 and pH 5.5 is 87 mM. Accordingly, ionic strength was changed for individual experiments with Sodium Chloride, Ammonium Sulfate and Sodium Acetate. The experiments related to change in ionic strength of solution was studied using, Brownian Microscopy to study the average cluster size and cluster volume fraction and Static Light Scattering for second virial coefficient of protein monomers.

The results of above experiments are shown in Figure 3-3(b)-(d). The following observations can be drawn from the results:

1. The average radius of clusters as shown in Figure 3-3(c) decreases as the ionic strength of protein solution increases. This trend is similar for various salts used.
2. The ratio of volume fraction of cluster to protein monomer in protein solution decreases as ionic strength is increased, shown in Figure 3-3(d).

The above results indicated that there is repulsion between the protein monomers, which results in decrease of cluster radius and this is seen for the volume fraction ratio as well. This is in contrary as addition of salts(electrolyte) leads to shielding of protein charge based on the Debye-Huckel Theory. Based on Debye-Huckel theory, as the ionic strength increase the Debye length or the length to how far the electrostatic effects of charged species have an effect, should decrease as ionic strength is increased. The Debye length for electrolytic solutions is inversely proportional to Ionic strength of solution. According to screening effects, the effect of charged species or here the charged RNase A, would

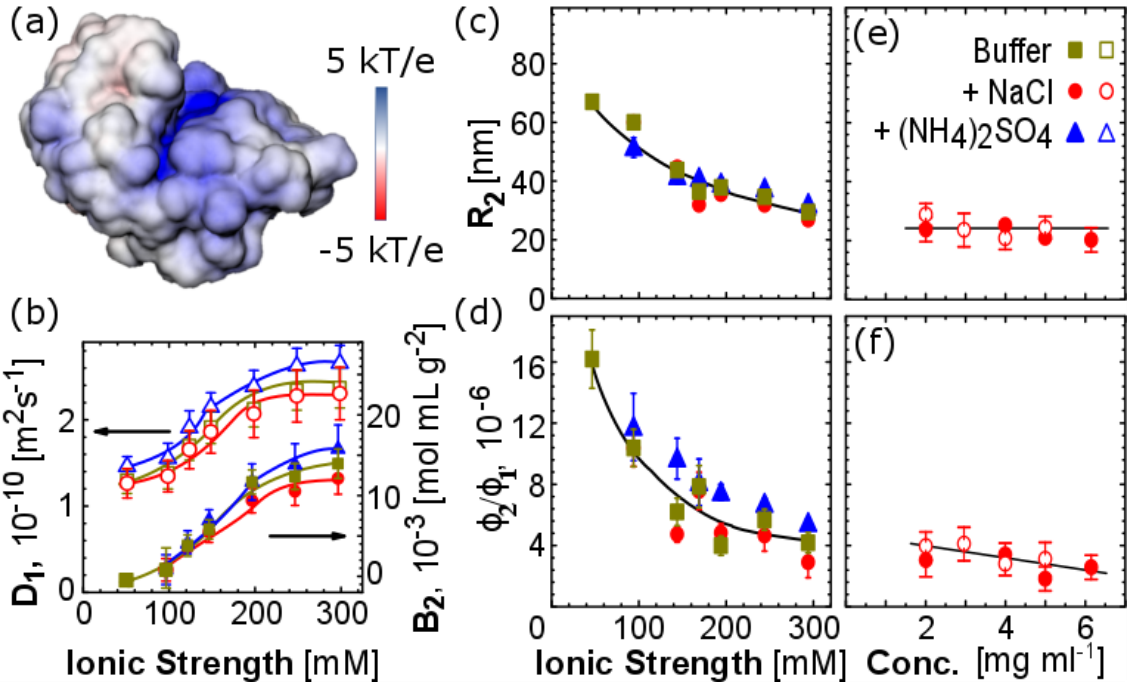

Figure 3-3. (a)Electrostatic potential at the solvent accessible surface of RNase A at pH 5.5 and 2 mg ml^{-1} (b), (c), (d)D_1, B_2, R_2, ϕ_2/ϕ_1 as function of Ionic strength (e) R_2 and cluster volume fraction at 288 mM ionic strength.

decrease in vicinity. This would produce results where the average radius would either stay constant or increase. In order to explain this disparity, the second virial coefficient(B_2) was measured using Static Light Scattering which is shown in Figure 3-3(b). There is increase in B_2 as the ionic strength is increased from lower range of 47 mM to 288 mM. This indicates that Protein monomer is more repulsive as the ionic strength is increased which is supported by increase in the Monomer Diffusivity which is found using Dynamic Light Scattering. The Diffusivity of monomer must increase; this is because of the repulsive characteristic of charged protein monomer at that particular pH. The trends as shown in the Figure 3-3(b)-(d) suggests that, cluster radius and cluster volume fraction are a function of ionic strength and independent of type of salts used based on the conditions set forth by experimentation and its applicability. The increase in B_2 and D_1 supports the decrease in

cluster radius and cluster volume fraction as the ionic strength increases. The two step nucleation theory states the interplay of transient dimers in formation of these clusters, and these dimers need to be close at certain orientation, which implies that increase in Monomer diffusivity decrease the life time of such transient dimers and leading to decrease in number of such clusters which eventually leads to decrease in cluster volume fraction. The electrostatic potential value of RNase A at pH 5.5 in a 100 mM sodium acetate buffer, was modelled using Adaptive Poisson-Boltzmann Solver available by PROPKA and the data obtained is depicted in Figure 3-3(a) using PyMOL. The pI of Ribonuclease A is 9.6 and at pH 5.5, the charge of protein is +7 and most of this charge as can be seen in the figure lies in the cleft of the protein, or the active site for the protein which explains for the repulsive behavior or positive second virial coefficient. This indicates that there is strong repulsion between the protein monomers. The decrease in volume fraction ratio at higher ionic strength can be explained because of the salting-in, i.e., the increase of solubility of proteins and colloids at increasing ionic strength. The decrease contradicts the trend of decreasing molecular repulsion at high ionic strength and suggests that other forces other than Coulomb are at play. This is a direct observation from the screening effect of ions. In literature, it is known that various ions bind to RNase A. The surface charge distribution as show in Figure 3-3(a) is positively charged, but since the protein tends to be more repulsive indicated by the increase in B_2 which implies that positive ions from the solution binds to the neutral surface of the protein as the ionic strength is increased, this binding is more. The binding of cations to largely positive surface of the protein is not favorable. Another possible explanation to this could be that the partially unfolded protein species are stabilized due to more binding of anions as ionic strength is increased which helps in

refolding and thus preventing the intermolecular interactions and hence decreasing the life time of the transient dimer species. This directly impacts the formation of cluster. As the ionic strength of solution is increased, the refolding of protein that were partially unfolded increases and hence exposure of various hydrophobic residues decreases and thus a decrease in cluster radius is seen. The Dilution experiments done at higher ionic strength of 288 mM and the results are shown in Figure 3-3(e)-(f). In previous dilution experiment done at 100 mM ionic strength, the cluster radius is constant and volume fraction ratio of cluster and protein monomer decreases as protein concentration is increased, a similar trend is seen in the case for higher ionic strength dilution experiments results. Since the experiment was done at higher ionic strength the average radius of cluster has dropped to around 25 nm, this drop is visible in volume fraction ratio as well. This indicates the importance of ionic strength in the role of cluster formation.

The formation of transient dimers is an interplay between the attractive and repulsive forces. Clusters are dense liquid in nature, and in such short separations the role of hydration and hydrophobic interactions play a key role in cluster stability. These forces can be grouped under water structuring forces. Hydration is due to water structuring at polar surface patches and augmented by presence of ions, Hydrophobic interactions are due to the water layering along the non-polar surface patches. Increase in concentration of ions leads to increase in hydration layers and hydrophobic repulsion at short separations and tend to destabilize the cluster phase. To test the role of such forces, Urea was used as an additive. Urea is known to destabilize the native structures of protein and addition in excess of 8M Urea leads to denaturing of protein. This happens because the various secondary structures are held due to the Hydrogen bonding present between them, and Urea

can come in between and break this Hydrogen bonding leading to disruption in conformation of the secondary structure. Urea interacts favorably with peptide backbone. Urea is known chaotropic agent and it accumulates in the vicinity of nonpolar amino acid residues disrupting the adjacent water structures. For experiments, RNase A concentration was kept at 2 $mgml^{-1}$ with Buffer as 100 mM Sodium Acetate, pH 5.5 and Urea concentration was varied from 0 M to 3 M (much below the denaturing concentration of 8M Urea). before analyzing the solutions using Brownian Microscopy and Static Light Scattering. All solutions were filtered using 0.2 μm Teflon filter.

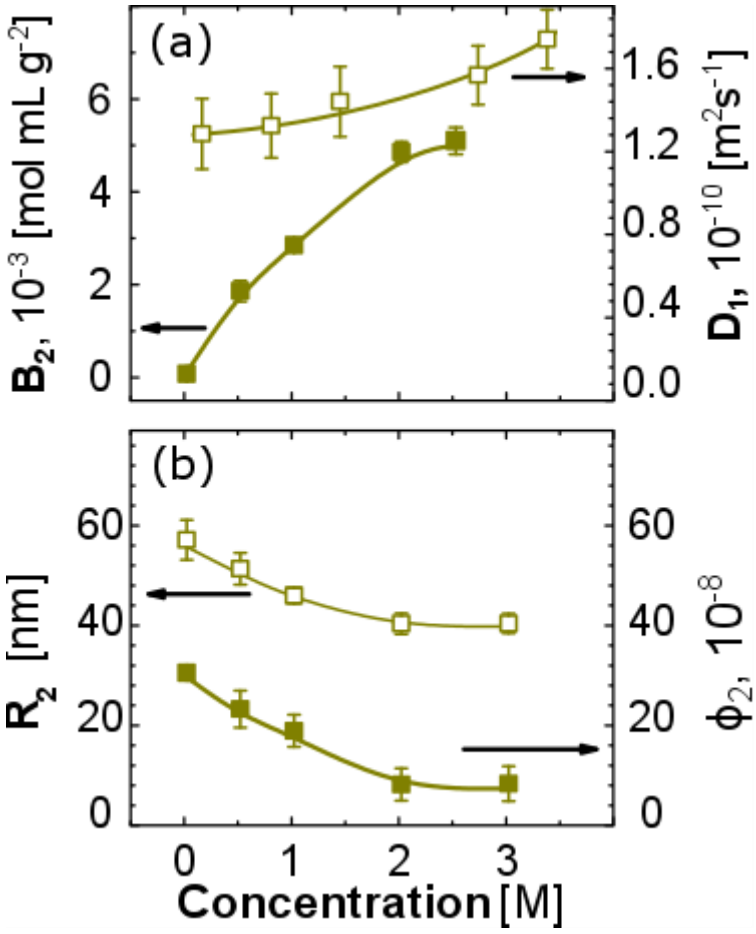

Figure 3-4. The role of hydrophobic interactions. 6 $mgml^{-1}$ RNase A solution in 0.1 M sodium acetate, pH 5.5 (a)B_2 and D_1 as a function of Urea concentration (b) Cluster size and Cluster volume fraction as a function of Urea concentration.

The results from the above experiment is shown in Figure 3-4. The following observations can be drawn from the result:

1. The average cluster radius decreases with increase in Urea concentration as shown in Figure 3-4(b).
2. The cluster volume fraction also decreases with increase in Urea concentration as shown in Figure 3-4(b).

The decreasing radius and volume fraction of clusters as Urea concentration increases can be explained from the chaotropic effect of Urea and its water structuring effects of Urea. The second virial coefficient(B_2) increases as the Urea concentration increases. This increase in B_2 also shows an increase in monomer diffusivity as the concentration of Urea increases in the protein solution. These results indicate the weakening of hydrophobic interactions and consistent with disruption of water structures around the nonpolar surfaces of amino acid residues which results in partial unfolding of protein.

We have till now studied the effects of ionic strength and effect of adding chaotropic agent, Urea in the formation of RNase A clusters. The structural conformation of protein has important effect in cluster formation. Partial unfolding of proteins might have impact in cluster formation. The partial unfolding of RNase A might be formed by breaking one of the four disulphide bonds. The protein in the native state has no inclination to form any dimers, as these are the most stable energy configuration, unless there is some partial unfolding the proteins might not interact. To test this hypothesis, experiments were done by heating the protein solution. This heating leads to breaking of disulphide bonds and an attempt is made to understand the role of disulphide bonds in formation of clusters for RNase A. For experiments, protein solutions were prepared in

100 mM Sodium Acetate buffer, pH 5.5. Heating of these solutions were done in 1 ml plastic cuvette, which can handle temperatures upto 100°C. The protein solutions were

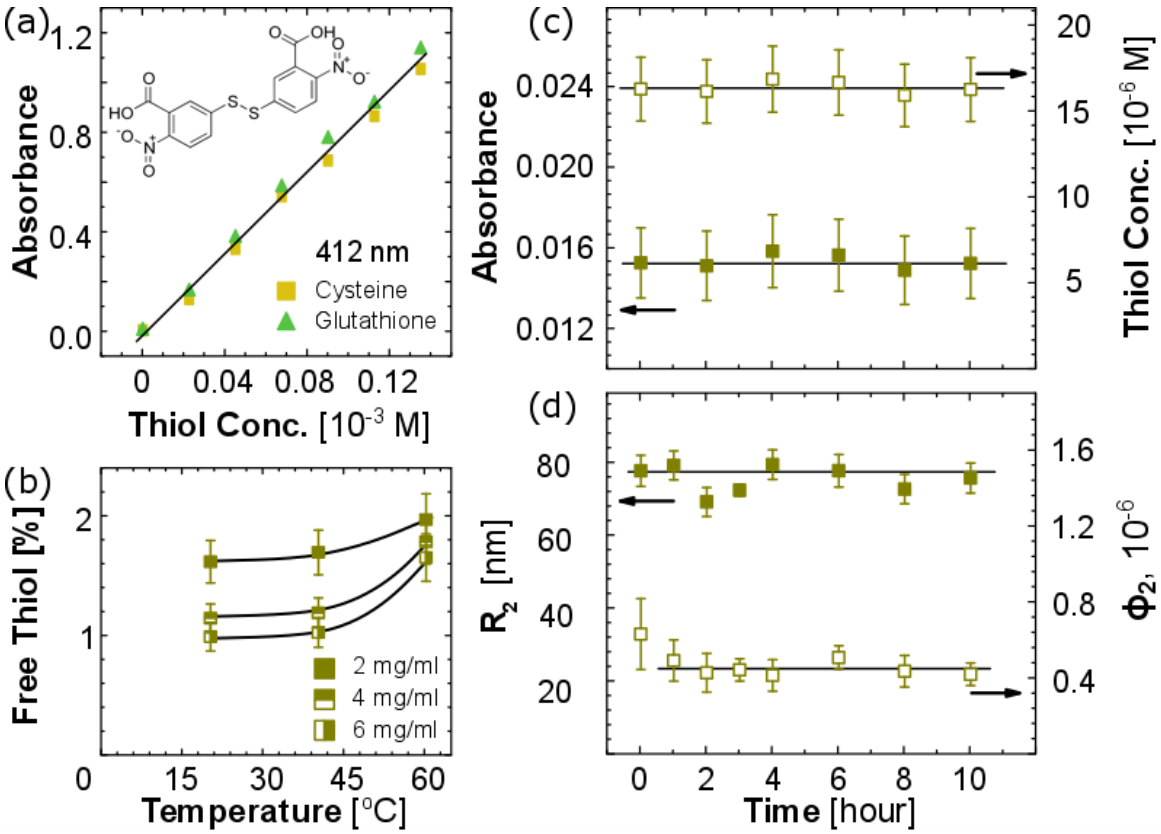

filtered using 0.2 um Teflon filters. Heating was done in water bath and protein solutions were heated for 30 minutes, later cooled before to room temperature before analysis.

Figure 3-5. (a) Calibration curve for Elman's Assay (b) Free thiol percentage as a function of temperature. RNase A, 6 mg ml^{-1}(c) Free thiol, absorbance as a function of time (d) Average cluster radius, volume fraction as a function of time.

From the results as shown in Figure 3-5(b), the percentage of broken disulphide bonds or free thiols present in the solution were quantified using the Elman's Assay, for different temperatures and various concentrations of RNase A in the solution. As the heating temperature is increased there is an increase in percentage of broken disulphide bonds. Then another set of experiment done at 6 $mgml^{-1}$ RNase A concentration, heated

to 60°C for 30 mins, and then cooled and analyzed for the stability of species from the heating of solution. The measurements were taken for a period of 10 hours. The graph 3-5(c) shows the concentration of the broken disulphide bonds do not change with time. The same trend is shown by average cluster radius and cluster volume fraction as shown in Figure 3-5(d). These results indicate that clusters formed is stable and their volume fraction or size do not change with time, or the cluster formation has reached a steady state region.

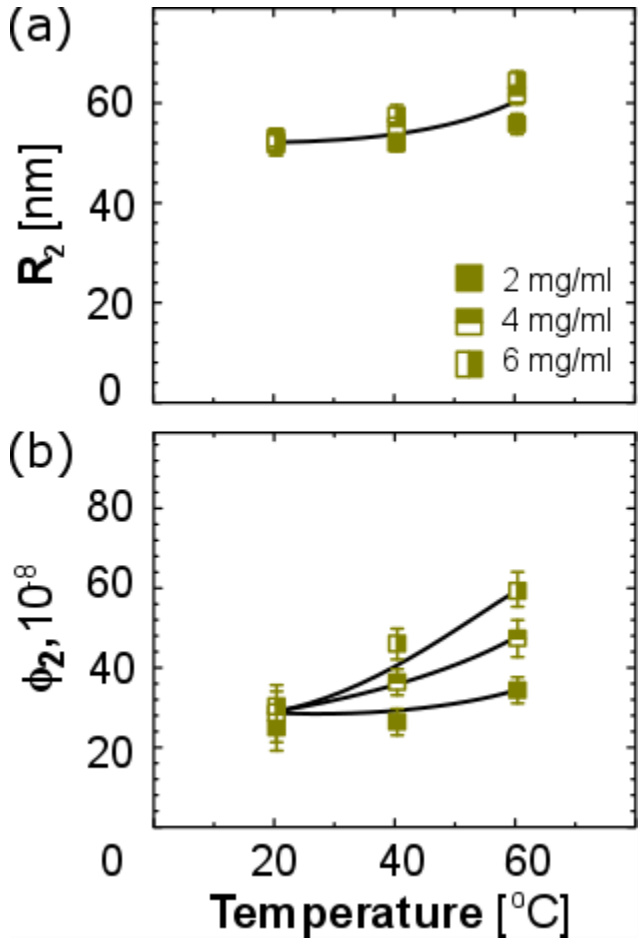

Figure 3-6. (a) Average Cluster radius as a function of temperature plotted for various protein concentrations. (b) Cluster Volume fraction as a function of temperature for different protein concentrations.

Heating leads to breaking of disulphide bonds. The effect of broken disulphide bonds on cluster radius and volume fraction is shown by Figure 3-6. There is a 25%

increase in average cluster radius and this increase in magnified for the case of volume fraction as the temperature is increased. The thermal denaturation temperature (T_M) for RNase A is around 80^{o}C, this means that at T_M fifty percent of the protein in the solution has unfolded. The high thermal denaturation temperature of RNase A is because of the presence of four disulphide bonds and has the ability to refold back into its native state. This high thermal endurance is unique to RNase A. The experimental conditions for

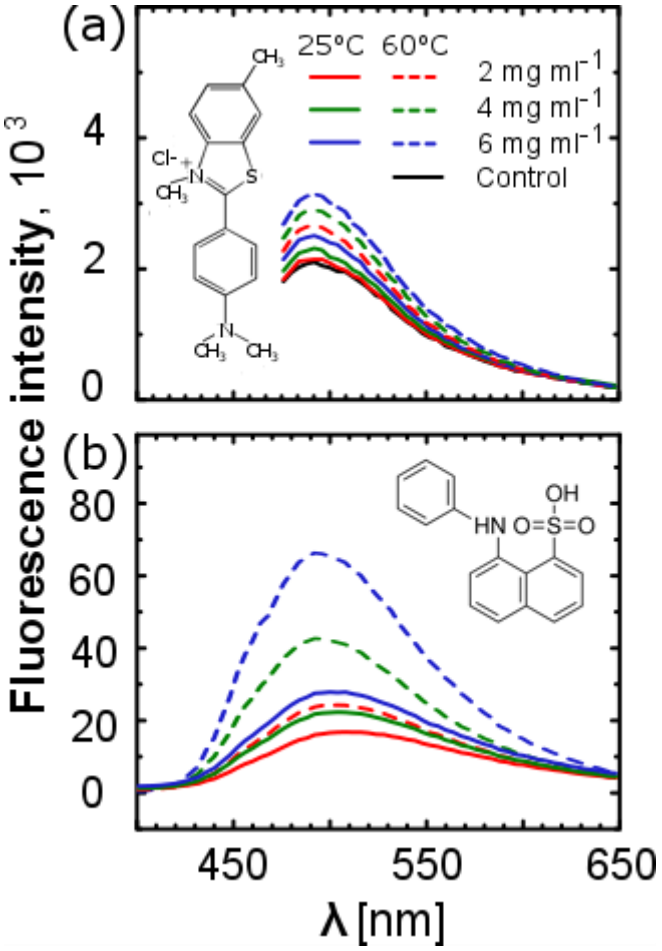

Figure 3-7. (a)Thiofalvin T assay (b) ANS assay

RNase A, were done in mild conditions. Heating to 60^{o}C which is below the denaturing midpoint temperature will not lead to complete unfolding of protein. This is also shown with the help of two assays, Thioflavin T (ThT) and ANS assays. The result for Figure 3-7(a) indicates that with respect to the native protein, heating the protein does not lead to

much change in protein conformation, but there is slight increase in intensity indicating partial unfolding of protein which exposes more hydrophobic residues. The data from ANS, shows that upon heating there is exposure of more non-polar groups which are generally hidden inside the protein core. Due to this ANS attaches strongly to the non-polar groups and gives a high intensity read out. This indicates the partial unfolding of protein. The reason for unfolding of protein upon heating can be attributed to breaking of disulphide bonds present in RNase A. Opening up the structure leads to more interactions between other protein entity through Hydrogen bonding or Vander Waals interactions. Partial unfolding of protein increases the tendency for proteins to interact and hence increases the life time of the transient dimer complexes. The increase in average size of cluster and volume fraction indicates that partial unfolding of proteins play an important role in cluster formation.

CHAPTER 4

CONCLUSION

Dense liquid droplets called Clusters have been seen in various protein solutions such as Lysozyme, Hemoglobin, Glucose Isomerase. These clusters play a vital role and acts as precursors to nucleation.

The study with Ribonuclease A showed the presence of such Mesoscopic clusters in the protein solutions even at very low concentrations. These clusters exist even in a very dilute protein concentration of 2 $mgml^{-1}$. With the help of Brownian Microscopy, the clusters size distribution was found out and showed the monodisperse nature of clusters. The average size ranges from 35 nm to 65 nm. The monodisperse nature helped us suggest that these are not aggregates. The fraction of volume occupied by these clusters are very small in range of 10^{-8} of the total volume. The cluster volume fraction, is a thermodynamically controlled parameter. The cluster volume fraction changes as the protein concentration is changed. The cluster volume fraction increases as the protein solution is diluted. This change suggests that these clusters react with the conditions of environment and not "dead" like the aggregates in general. The first part of experiments to confirm the presence of clusters.

After confirming the existence of these stable species, we studied the factors that might affect or control the formation of clusters. RNase A, at pH 5.5 is a highly charged protein. It is known from previous work, that ionic strength of the solution changes the interactions between the individual proteins. The effect of ionic strength on cluster formation was probed. It was found that the clusters of RNase A become less stable as the ionic strength of the solution is increased. The range of ionic strength studied is from 0.05

M to 0.3 M. This was done by either increasing the concentration of sodium acetate, or to add sodium chloride or Ammonium Sulphate to the buffer system. The cluster volume fraction also drops indicates that at higher ionic strength the cluster system become unstable. A possible explanation might be the salting in at lower ionic strength. As a result, the protein dissolves back into the solution and hence falls apart. This study was complemented with the measurement of second virial co-efficient, and the positive values indicated that protein monomers are more repulsive at higher ionic strength. The monomer diffusivity also increases accordingly. In the two step nucleation theory, these clusters are formed from the transient dimers. The lifetime of these dimers are in the order of microseconds and inversely proportional to Monomer Diffusivity. Here the monomer diffusivity increases and hence life time of these clusters drop thus the cluster volume fraction drops with increase in ionic strength. This increase in repulsive behavior might be attributed to the binding of ions to RNase A. Binding of anions to RNase A refolds the partially unfolded structures, which leads to decreased interactions between protein molecules. This leads to drop in cluster radius and cluster volume fraction as concentration of anions is increased. Thus ionic strength of the solution is a deciding factor in the stability of these clusters.

The role of a chaotropic agent, Urea was studied as well. Urea disrupts the water structuring forces such as hydrogen bonding at Urea concentrations lower than 8M, above which leads to protein denaturation. Protein interacting with Hydrogen bonds or interactions between hydrophobic residues, gets disturbed due to Urea. Protein being highly charged and when these attractive forces are disrupted the stability of clusters decreases with increasing Urea concentration. The experiments conducted showed that

average cluster size and volume fraction drop as the Urea concentration increases from 0 M to 3 M. Similar experiments were done to measure the second virial coefficient and monomer diffusivity. The proteins become less attractive as the Urea concentration is increased.

The structural flexibility of RNase A, leads to the formation of domain swapped dimers. RNase A is highly flexible and we were interested to study the contributions of this flexible protein in cluster formation. Heating was used as one of the methods to partially unfold the protein with the idea of breaking a disulphide bond. RNase A has a high denaturation midpoint temperature, which tells about the high stability of protein. With the help of Brownian Microscopy, the average cluster size and volume fraction was determined. The monodisperse nature suggests that we are avoiding any aggregation. The proteins were heated to 60^{o}C for 30 minutes and then later cooled down to room temperature. It was observed that the cluster formed are highly stable and their cluster size and volume fraction do not change with time suggesting that we are in a steady state. The increase in temperature leads to increase in cluster radius and cluster volume fraction. The molecular picture of these clusters were viewed with the help biological assays. Elman's Assay helped in quantification of broken disulphide bonds. This showed that percentage of broken disulphide bonds in the solution increases with heating. Other complementary assays such as ThT and ANS showed the increase in unfolding of proteins with heating. These when grouped with average cluster size and volume fractions, indicates that partial unfolding of RNase A helps in formation of more stable clusters. This is due to the opening of hydrophobic residues generally hidden inside and interacting with other protein through van der Waals forces. A drawback of this result is the formation of oligomers due to

heating, oligomeric species are not clusters and hence as a future work these must be separated from the solution with the help of size exclusion chromatography and tested again.

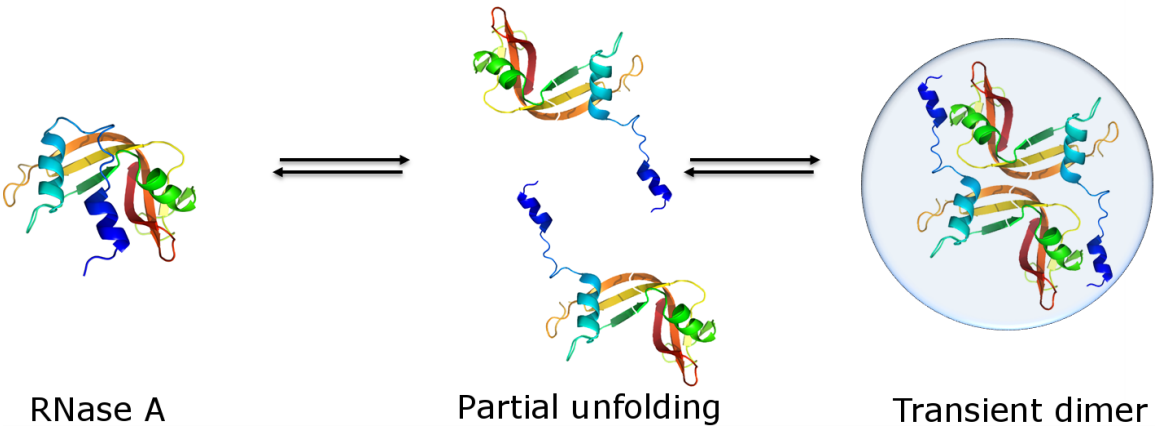

Figure 4.1: Schematic representation for the formation of transient species.

The model proposed suggests that partial unfolded structures of RNase A exist in the solution in equilibrium with the protein monomer, and these partially unfolded structures interacts due to increased interactions between the individual unfolded structures leading to the formation of transient dimers. The partial unfolding of RNase A exposes the hydrophobic residues leading to stronger interaction due to the van der Waals' interactions and hence increasing the life time of transient species. This would lead to higher formation of clusters in the protein solutions.

To summarize, the experiments shows the existence of RNase A clusters even in dilute protein concentrations. Stability of clusters are related to a number of parameters such as Ionic strength, pH, nature of interactions and structure of protein molecule.

CHAPTER 5

FUTURE WORK

It is proposed that the formation of clusters in RNase A is due to the partial unfolding of protein. This unfolding is done with the help of heating. Heating does help in partial unfolding, via breaking of disulphide bonds, but is a high possibility of formation of RNase A oligomers. These oligomers are highly stable and it is essential to separate these oligomeric species from the protein solutions and later see them under the Nanosight. The aim of this experiment is to confirm definitely that existence of RNase A clusters. The separation of these oligomers can be done with the help of size exclusion chromatography. Initial experiment was done to separate a heated RNase A sample of 7.8545 $mgml^{-1}$ heated to 60^{o}C for 50 minutes in buffer of 0.1 M Sodium Acetate, pH 5.5. The running buffer for Size exclusion chromatography is 0.1 M Sodium Acetate, pH 5.5. The SEC media was purchased from GE, Superdex 200 and packed into the column. Column was washed with

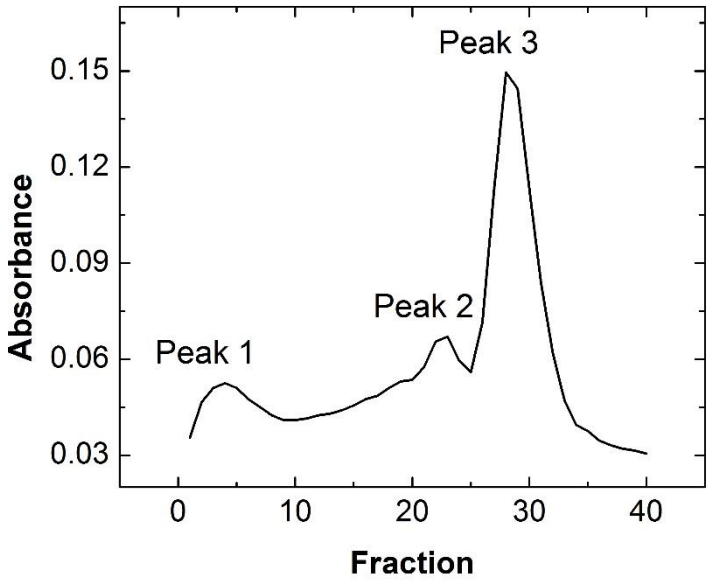

Figure 5-1. Elution profile of RNase A sample after Size Exclusion Chromatography

the Buffer till the Absorbance reaches a constant value. A sample volume of 0.5 ml was injected into the system and sent into the Chromatography column. The absorbance reading is checked and the eluted solution is collected according to the absorbance reading. The Figure 5-1, represent the SEC profile of eluted fraction. In Size exclusion chromatography, the larger aggregates diffuse faster and hence come out earlier. Peak 1 represents the larger aggregates, Peak 2 represent the small oligomers as the peak is next to Peak 3 which is for the protein monomer.

After purification of protein from the SEC, which is shown as Peak 3 in Figure 5-1, a native electrophoresis gel must be run. This should be done to confirm the existence of just proteins. Initial experiments were done with three RNase A samples at 40 mg ml^{-1}, with Sample 1 as not heated, Sample II heated to 60^{o}C and Sample III heated to 100^{o}C in

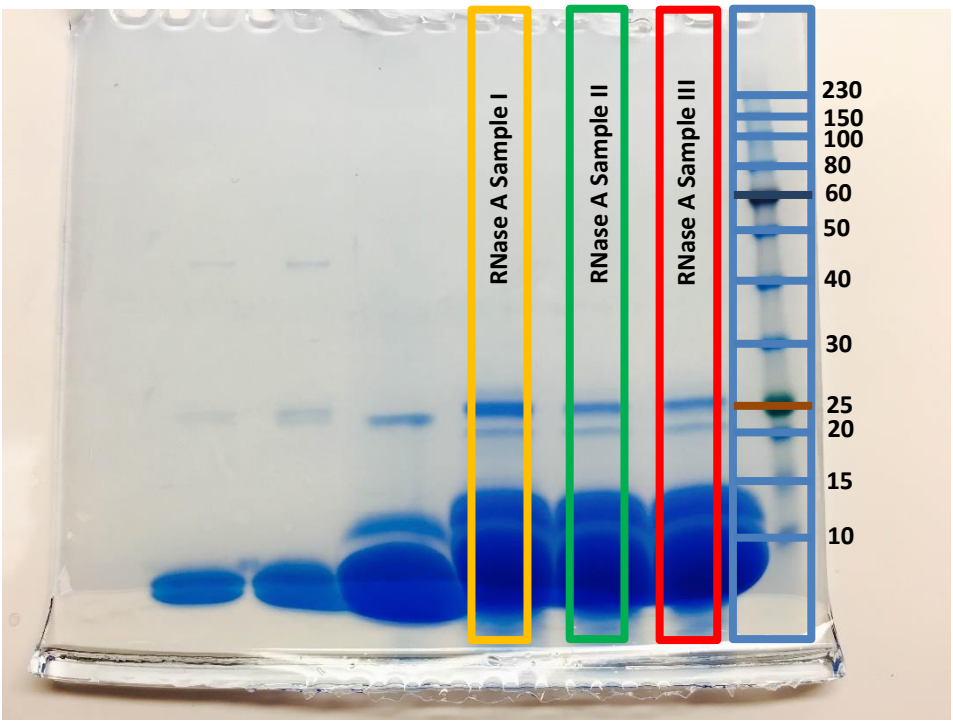

Figure 5-2: Electrophoresis Gel of RNase A

presence of 100 mM Sodium Acetate, pH 5.5 buffer. When loading the samples into the gel, it was mixed in 1:1 ratio of Laemmli Buffer (Tris-HCl, pH 6.8, 20% v/v glycerol, Mercaptoethanol and bromophenol blue as a dye). The electrolyte used was 4% w/v SDS buffer. The voltage was set at 120V and ampere should be around 0.05 A, to prevent heating. The fractions of protein separate into various bands depending upon the molecular weight of the aggregate as the voltage is applied and later stained with Coomaisse blue staining method. The Figure 5-2, indicates the presence of oligomers and higher aggregates in RNase A.

Another important aspect is to simulate the events of cluster formation. The experiments show the partial unfolding of RNase A, which aids in formation of cluster. A theoretical explanation must also be presented to show the energy profile of various unfolding stages of RNase A. It has also been shown that breaking of disulphide bonds leads to protein unfolding. There are four disulphide bonds in RNase A and calculation of bond energies of individual disulphide bonds needs to be calculated and check how it effects the protein structure.

REFERENCES

1. Hunter, M. S.; DePonte, D. P.; Shapiro, D. A.; Kirian, R. A.; Wang, X.; Starodub, D.; Marchesini, S.; Weierstall, U.; Doak, R. B.; Spence, J. C. H.; Fromme, P. *Biophysical Journal* **2011**, 100, 198.

2. Mueller, M., S. Jenni, and N. Ban. "Strategies for Crystallization and Structure determination of very large Macromolecular Assemblies" *Curr. Opin. Struct. Biol*. **2007** 17:572–579.

3. Drenth, J. "Principles of Protein X-ray Crystallography", *Springer Science*, New York **2007.**

4. Jensen, P. K., Lee, C. S., & King, J. A. "Temperature Effects on Refolding and Aggregation of a Large Multimeric Protein Using Capillary Zone Electrophoresis", *Anal. Chem.* **1998** 70(4), 730–736.

5. Vottariello, F., Giacomelli, E., Frasson, R., Pozzi, N., De Filippis, V., & Gotte, G. "RNase A oligomerization through 3D domain swapping is favoured by a residue located far from the swapping domains". *Biochimie*, **2011**, 93(10), 1846–1857.

6. Pfefferkorn, C. M., Mcglinchey, R. P., & Lee, J. C. "Effects of pH on aggregation kinetics of the repeat domain of a functional Amyloid Pmel17". *PNAS* 107(50) **2010**, 21447–21452

7. Risso, P. H., Borraccetti, D. M., Araujo, C., Hidalgo, M. E., & Gatti, C. A. "Effect of temperature and pH on the aggregation and the surface hydrophobicity of bovine RNase A-casein", *Colloid and Polymer Science*, 286(12) **2010**.

8. Bennion, B. J., & Daggett, V. "The molecular basis for the chemical denaturation of proteins by urea", *PNAS* **2003**(Track II) 5142–5147.

9. Gibbs, J. W. Trans Connect Acad Sci **1876**, 3, 108.

10. Gibbs, J. W. Trans Connect Acad Sci **1878**, 3, 343.

11. Vekilov PG. "Nucleation. Crystal growth & design". **2010**;10(12):5007-5019. doi:10.1021/cg1011633.

12. Vekilov, P. G. *NIH Public Access* **2011**, 10(12), 5007–5019.

13. Asherie N, Lomakin A, Benedek GB. "Phase diagram of colloidal solutions". *Phys. Rev. Lett* **1996**;77(23):4832–4835. [PubMed: 10062642]

14. Mutaftschiev, B. Nucleation theory. In: Hurle, DTJ., editor. Handbook of crystal growth. Vol. Vol. I. Amsterdam: *Elsevier*; **1993**. p. 189-247.

15. Turnbull, D. and Fisher, J.C. J. *Chem. Phys*. **1949**, 17, 71.

16. Pan W, Kolomeisky AB, Vekilov PG. "Nucleation of ordered solid phases of protein via a disordered high-density state: Phenomenological approach". *J. Chem. Phys* **2005**; 122:174905. [PubMed: 15910067]

17. Yau, S. T.; Vekilov, P. G. *Nature* **2000**, 406, 494.

18. Pan W, Vekilov PG, Lubchenko V. "The origin of anomalous mesoscopic phases in protein solutions". *J. Phys. Chem. B* **2010**; 114:7620–7630. [PubMed: 20423058]

19. Vekilov, PG.; Pan, W.; Gliko, O.; Katsonis, P.; Galkin, O. "Metastable mesoscopic phases in concentrated protein solutions." In: Franzese, G.; Rubi, M., editors. Lecture Notes in Physics, vol. 752: "Aspects of Physical Biology: Biological Water, Protein Solutions, Transport and Replication". *Heidelberg: Springer*; **2008**. p. 65-95

20. Li, Y.; Lubchenko, V.; Vorontsova, M. A.; Filobelo, L.; Vekilov, P. G. *J Phys Chem B* **2012**, 116, 10657.

21. Pan, W.; Galkin, O.; Filobelo, L.; Nagel, R. L.; Vekilov, P. G. *Biophys J* **2007**, 92, 267.

22. Pan W, Vekilov PG, Lubchenko V. "The origin of anomalous mesoscopic phases in protein solutions". *J. Phys. Chem. B* **2010**; 114:7620–7630

23. Liu, Y., Gotte, G., Libonati, M., & Eisenberg, D. "Structures of the two 3D domain-swapped RNase A trimers", *John Wiley and Sons* **2011**, 371–380.

24. Vottariello, F., Giacomelli, E., Frasson, R., Pozzi, N., De Filippis, V., & Gotte, G . "RNase A oligomerization through 3D domain swapping is favoured by a residue located far from the swapping domains", *Biochimie* **2011**, 93(10), 1846–1857.

25. Raines, R. T. "Ribonuclease A. Chem Review", *American Chemical Society* **1998**.

26. Liu, Y., Gotte, G., Libonati, M., & Eisenberg, D. "Structures of the two 3D domain-swapped RNase A trimers", **2002,** 371–380.

27. Miller, K. H., Karr, J. R., & Marqusee, S. "A Hinge Region cis-Proline in Ribonuclease A Acts as a Conformational Gatekeeper for C-Terminal Domain Swapping", *Journal of Molecular Biology* **2010**.

28. Liu, Y., Hart, P. J., Schlunegger, M. P. and Eisenberg, D. "The crystal structure of a 3D domain-swapped dimer of RNase A at 2.1-A° resolution". *Proc. Natl. Acad. Sci*. **1998** U.S.A. 95, 3437–3442

APPENDIX

6-1. Binding of Chloride and Sulphate ions to Ribonuclease A

At isoelectric point, RNase A has 12 negative and 12 positive charges

Negative Charges: 11 carboxylate ions, 1 phenolic ion

Positive Charges: 4 arginine residues, 8 amino groups

Neutral: 4 imidazole of Histidine, 3 amino groups

Reaction of binding of ions:

$$PN + H^+ \rightarrow PNH^+$$

$$PNH^+ + A^- \rightarrow PNHA,$$

Where, PN = unprotonated,

PNH^+ = protonated,

PNHA = complex forms.

For a set of 'n' equivalent sites of a protein, average number of ions bound per mole of protein, X_A;

$$X_A = \frac{k'_A C_A n}{1 + k'_A C_A + \frac{1}{k'_H C_H}},$$

Where, k'_A and k'_H are the intrinsic association constants for binding of ions and hydrogen ions, C_A and C_H are concentrations of anions and hydrogen ions.

For larger C_H,

$$X_A = \frac{k'_A C_A n}{1 + k'_A C_A},$$

Chloride Ions:

"At isoelectric point, no Cl^- ions are bound, at pH 4.4, all amino groups and imidazole groups are charged the binding is 2 moles per mole of RNase A"

- At isoionic point, 11 of the 18 nitrogen center are protonated, yet no Cl^- ions binds.
- When all amino groups and 1 out of 4 imidazole group is protonated, a small amount of Cl^- ions bind.
- 2 moles bind when 4 imidazole groups are charged. Association constants for the 2 sites are nearly same.

These indicates that, Cl^- ions binds to the Imidazole group in the Histidine and Amino group of Lysine.

Sulphate ions:

*"*At pH 4.5, when all nitrogen centers are protonated, number of SO_4^{2-} ions bound is 2.3 moles per mole of 2 moles of RNase A."

- At pH 6.8, Lysine and Arginine should be protonated, but not the Imidazole group of Histidine (localized electrostatics play an important role)
- At lower C_H or at higher pH, binding of SO_4^{2-} ions is much higher compared to Cl^- ions

Sulfate ions binds to the Imidazole group in the Histidine and Amino group of Lysine. Binding happens when a cluster of such protonated groups are found.

Possible Cluster of positive charges:

1. His 48, His 105 + Lysine or Arginine (as these are already held in position by a pair of di-sulphide bonds by Cysteine residues 40,96 and 58,111)
2. His 12, His 119 + Lysine or Arginine
3. His 12, His 119 are located at the end, not restricted by di-sulphide bonds, and can be brought into close proximity of His 48, His 105

6-2. Activity of Ribonuclease A

RNase A uses acid/base catalysis to speed up RNA hydrolysis. This occurs in the active site which is found in the cleft of RNase A and is the location of the chemical change in bound substrates. Subsites lining the active site cleft are important to the binding of single stranded RNA. Large quantities of positively charged residues, such as Lys7, Arg10, Arg39, and Lys41, and Lys66, recognize the negative charge on the phosphate back bone of the RNA strand.

RNase A catalyzes the cleavage of the Phosphodiester bonds in two steps: the formation of the pentavalent phosphate transition state and subsequent degradation of the 2’3’ cyclic phosphate intermediate using three main catalytic residues (His12, Lys41, and His119 and His12, Lys41, and His119 with substrate present). An important part of the reaction is the ability of histidine (His 12 and His119) to both accept and donate electrons, allowing these histidines to be an acid or a base, making the reaction pH dependent.

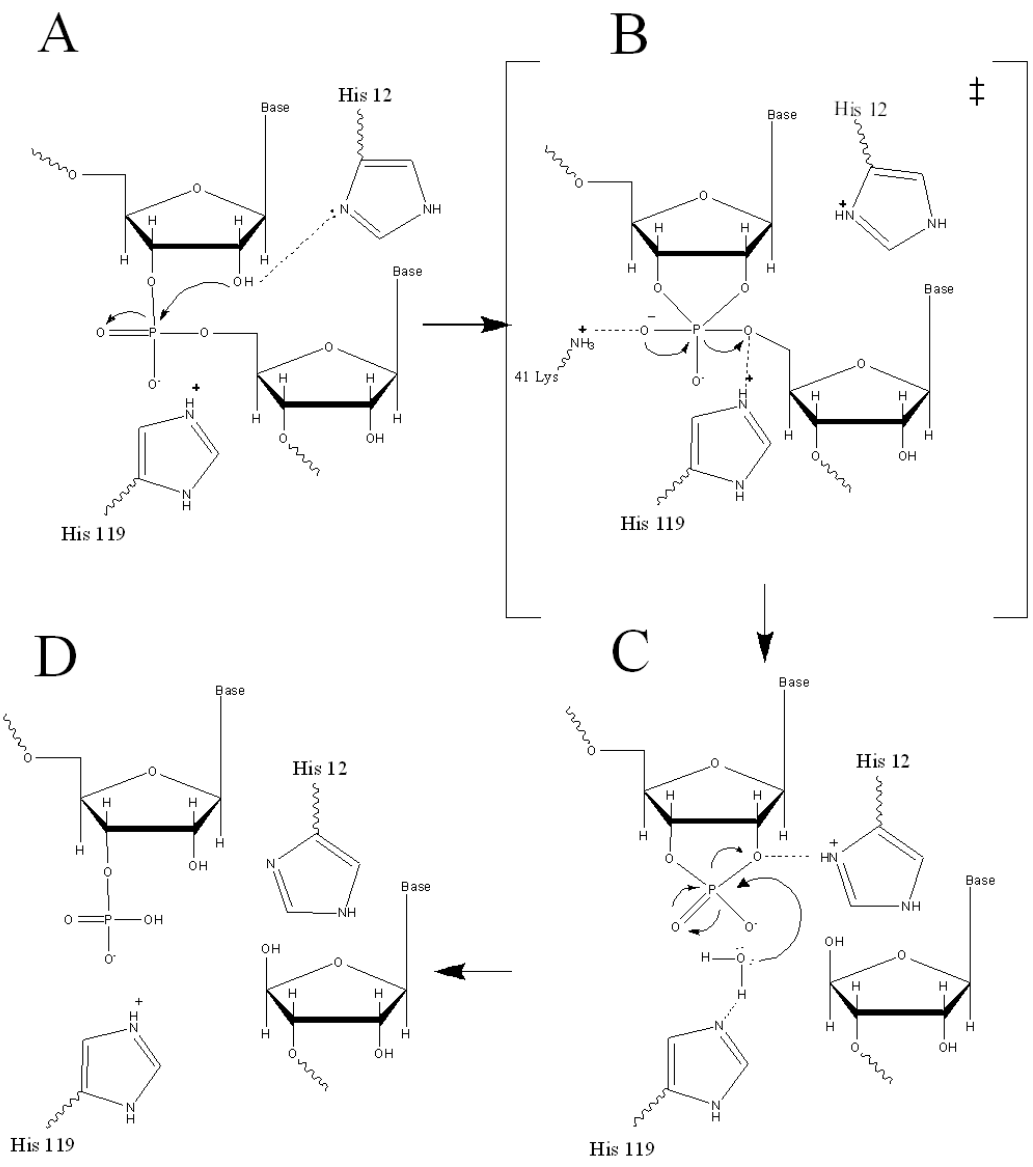

Figure A.1. RNase A Catalysis. (a) Initial attack of 2'hydroxyl stabilized by His12. (b) Pentavalent phosphorous intermediate. (c) 2'3' cyclic intermediate degradation. (d) Finished products: Two distinctive nucleotide sequences

RNA hydrolysis begins when His12 abstracts a proton from the 2’ OH group on RNA; thus, assisting in the nucleophilic attack of the 2’ oxygen on the electrophilic phosphorus atom. A transition state is then formed, having a pentavalent phosphate,

which is stabilized by the positively charged amino group of Lys41 and the main chain amide nitrogen of Phe120. His119 then protonates the 5' oxygen on the ribose ring and the transition state falls to form a 2’3’cyclic phosphate intermediate.

In a secondary and separate reaction, the 2’,3’ cyclic phosphate is hydrolyzed to a mixture of 2'phosphate and 3' hydroxyl. His12 donates a proton to the leaving group of this reaction, the 3’ oxygen of the cyclic intermediate. Simultaneously, His-119 abstracts the proton from a water molecule, activating it for nucleophilic attack. The activated water molecule attacks the cyclic phosphate causing the cleavage of the 2'3’ cyclic phosphate intermediate. The truncated nucleotide is then released with a 3’ phosphate z

6-3. Viscosity measurements

The indicated solution was prepared and then filtered using a 0.22 um Teflon filter. The 400 nm latex beads were used and one microliter of the it was mixed in the solution and analysed using Dynamic light scattering.

Using CONTIN, the values of Tau(ms), was found out and Diffusivity $(D) is \frac{1}{\tau.q^2}$.Using Stokes Einstein equation for a known value of radius and calculated diffusivity, Viscosity is given by $(\gamma) = \frac{k_B T}{6\pi D r}$, where T is the temperature, D is the diffusivity, r is the radius of the latex beads.

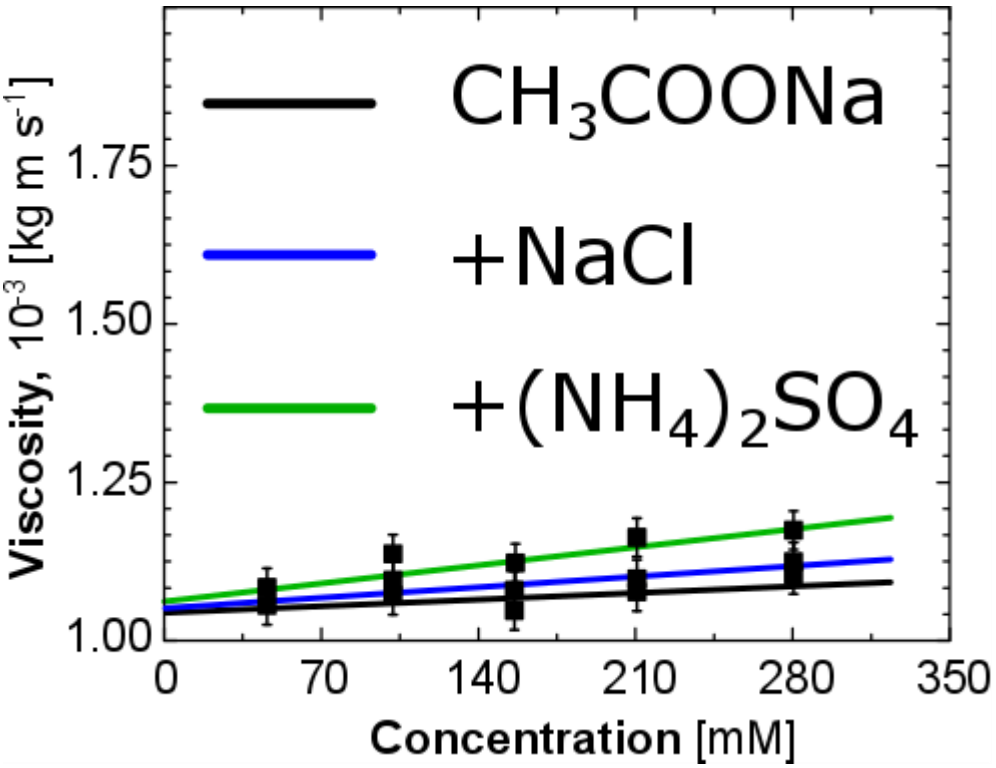

Figure A-2. Viscosity of solutions as indicated by colored lines.